

Effectiveness of Ammonium Ion in Low salinity Waterflooding in Shaly-sandstone
Reservoir



A Thesis Submitted in Partial Fulfillment of the Requirements
for the Degree of Master of Engineering in Georesources and Petroleum Engineering
Department of Mining and Petroleum Engineering
Faculty of Engineering
Chulalongkorn University
Academic Year 2018
Copyright of Chulalongkorn University

ประสิทธิภาพของแอมโมเนียมไอออนในกระบวนการฉีดอัดน้ำความเค็มต่ำในแหล่งกักเก็บหินทรายปน
หินดินดาน



วิทยานิพนธ์นี้เป็นส่วนหนึ่งของการศึกษาตามหลักสูตรปริญญาวิทยาศาสตรมหาบัณฑิต
สาขาวิชาวิศวกรรมทรัพยากรธรณีและปิโตรเลียม ภาควิชาวิศวกรรมเหมืองแร่และปิโตรเลียม
คณะวิศวกรรมศาสตร์ จุฬาลงกรณ์มหาวิทยาลัย
ปีการศึกษา 2561
ลิขสิทธิ์ของจุฬาลงกรณ์มหาวิทยาลัย

Thesis Title Effectiveness of Ammonium Ion in Low salinity
Waterflooding in Shaly-sandstone Reservoir
By Mr. Hung Vu Quoc
Field of Study Georesources and Petroleum Engineering
Thesis Advisor FALAN SRISURIYACHAI, Ph.D.

Accepted by the Faculty of Engineering, Chulalongkorn University in Partial
Fulfillment of the Requirement for the Master of Engineering

..... Dean of the Faculty of Engineering
(Professor SUPOT TEACHAVORASINSKUN, D.Eng.)

THESIS COMMITTEE

..... Chairman
(Assistant Professor JIRAWAT CHEWAROUNGROAJ, Ph.D.)

..... Thesis Advisor
(FALAN SRISURIYACHAI, Ph.D.)

..... Examiner
(Associate Professor DAWAN WIWATTANADATE, Ph.D.)

..... External Examiner
(Monrawee Pancharoen, Ph.D.)

ชง วุ คุวก : ประสิทธิภาพของแอมโมเนียมไอออนในกระบวนการฉีดน้ำความเค็มต่ำในแหล่งกักเก็บหินทรายปนหินดินดาน. (Effectiveness of Ammonium Ion in Low salinity Waterflooding in Shaly-sandstone Reservoir) อ.ที่ปรึกษาหลัก : อ. ดร.ฟ้าลั่น ศรีสุริยชัย

การฉีดอัดน้ำความเค็มต่ำได้ถูกทำการศึกษาอย่างแพร่หลายเนื่องจากเป็นวิธีการเพิ่มผลผลิตน้ำมันที่มีต้นทุนต่ำ วิธีดังกล่าวจะก่อให้เกิดการเปลี่ยนสมดุลของพื้นผิวหิน น้ำมัน และน้ำที่อยู่ล้อมรอบ ส่งผลให้เกิดการเปลี่ยนแปลงความเปียกของพื้นผิวหินผ่านกลไกการแทนที่ของไอออนหลายชนิด ในการศึกษาที่แอมโมเนียมไอออนได้ถูกเติมลงไปใต้น้ำจืดเพื่อส่งเสริมให้เกิดกลไกการแทนที่ของไอออนหลายชนิดในแหล่งกักเก็บน้ำมันแบบหินทรายปนหินดินดาน หินทรายปนหินดินดานถูกเลือกใช้ในการศึกษานี้เนื่องจากหินดังกล่าวอุดมไปด้วยแคลเซียมและแมกนีเซียมไอออนซึ่งเป็นส่วนประกอบของดินเหนียวและสามารถถูกแทนที่ด้วยแอมโมเนียมไอออนในระหว่างกลไกการแทนที่ของไอออนหลายชนิด การทดสอบด้วยการกวนสาร การทดสอบการไหลซึมด้วยแรงตามธรรมชาติ และการทดสอบด้วยการแทนที่ของไหล ได้ถูกจัดทำขึ้นเพื่อศึกษาผลกระทบของแอมโมเนียมไอออนในน้ำความเค็มต่ำที่อาจส่งผลประโยชน์ต่อกระบวนการผลิตน้ำมัน

จากการทดลองสามารถสังเกตได้ว่าแอมโมเนียมไอออนซึ่งเป็นไอออนที่ไม่มีอยู่บนเนื้อหินสามารถถูกดูดซับได้อย่างง่ายดายเพื่อแทนที่ไอออนประจุสองบวก อย่างไรก็ตามแอมโมเนียมไอออนมีแนวโน้มที่จะแทนที่แคลเซียมไอออนมากกว่าแมกนีเซียมไอออนบนพื้นผิวของดินเหนียว การเติมโพแทสเซียมไอออนลงไปในการละลายที่มีแอมโมเนียมไอออนอยู่แล้วส่งผลให้เกิดการเปลี่ยนแปลงความชอบในการแทนที่แคลเซียมไอออนไปเป็นการแทนที่แมกนีเซียมไอออน เนื่องจากแมกนีเซียมไอออนสามารถตรึงน้ำมันไว้บนผิวหินได้อย่างแน่นหนาซึ่งเป็นผลมาจากขนาดไอออนที่เล็กกว่าแคลเซียมไอออน แอมโมเนียมไอออนจึงจัดได้ว่ามีศักยภาพที่ดีกว่าโพแทสเซียมไอออนในการผลิตน้ำมัน ผลการศึกษาจากการทดสอบการไหลซึมด้วยแรงตามธรรมชาติ และการทดสอบด้วยการแทนที่ของไหลยืนยันว่าแอมโมเนียมสามารถใช้ในการเพิ่มผลผลิตน้ำมันในแหล่งกักเก็บแบบหินทรายปนหินดินดานได้ อย่างไรก็ตามการเตรียมสารละลายแอมโมเนียมไอออนจะต้องเตรียมให้สารละลายมีแนวโน้มเพื่อการแทนที่แคลเซียมไอออนมากกว่าแมกนีเซียมไอออนเนื่องจากน้ำมันที่ถูกตรึงไว้ด้วยแคลเซียมไอออนสามารถถูกผลิตได้ง่ายกว่าน้ำมันที่ถูกตรึงไว้ด้วยแมกนีเซียมไอออน

ในการศึกษานี้ สารละลายแอมโมเนียมคลอไรด์บริสุทธิ์และและสารละลายองค์ประกอบรวม แอมโมเนียม แคลเซียม และโซเดียม ในอัตราส่วน 40 20 และ 40 ตามลำดับ ที่ความเข้มข้นในส่วนในล้านส่วน แสดงให้เห็นถึงศักยภาพในการเพิ่มการผลิตน้ำมัน อย่างไรก็ตามสารละลายองค์ประกอบรวม แอมโมเนียม แคลเซียม และ โซเดียม ในอัตราส่วน 40 20 และ 40 น่าจะเป็นกรณีที่เหมาะสมกับแหล่งน้ำมันที่มีอยู่เนื่องจากโซเดียมไอออนสามารถผสมรวมกับไอออนชนิดอื่นในสูตรน้ำที่อัตราส่วนค่อนข้างสูง ปริมาณการใช้น้ำจืดเพื่อการเจือจางจึงลดลงจากเงื่อนไขการทดลองในการศึกษานี้พบว่าตรรกะการผลิตน้ำมันจากการใช้แอมโมเนียมไอออนสามารถเพิ่มขึ้นได้ถึง 26 เปอร์เซ็นต์

จุฬาลงกรณ์มหาวิทยาลัย
CHULALONGKORN UNIVERSITY

สาขาวิชา	วิศวกรรมทรัพยากรธรรมชาติและปิโตรเลียม	ลายมือชื่อนิสิต
ปีการศึกษา	2561	ลายมือชื่อ อ.ที่ปรึกษาหลัก

6071208621 : MAJOR GEORESOURCES AND PETROLEUM ENGINEERING

KEYWORD: ENHANCED OIL RECOVERY, LOW SALINITY WATERFLOODING MULTI-COMPONENT ION EXCHANGE
 AMMONIUM ION SHALY-SANDSTONES

Hung Vu Quoc : Effectiveness of Ammonium Ion in Low salinity Waterflooding in Shaly-sandstone Reservoir.

Advisor: FALAN SRISURIYACHAI, Ph.D.

Low Salinity Waterflooding (LSWF) has been intensively studied worldwide as it is a low-cost technique. By injecting water with very low salinity compared to formation water in the reservoir, the method changes equilibrium between rock surface, oil and surrounding water, causing wettability alteration through Multi-component Ion Exchange (MIE) mechanism. In this study, ammonium ion is added into low salinity water to facilitate the MIE mechanism in shaly-sandstones reservoir. Experiments are performed with shaly-sandstone rock as it contains both calcium and magnesium ions as part of clays and ammonium ion can express its potential by triggering MIE mechanism. Stirring test, spontaneous imbibition test and coreflooding test are performed to research the effects of ammonium ion in low salinity water that could generate positive results in oil recovery mechanism.

From the experiments, it can be observed that ammonium ion is a foreign ion that can be easily adsorbed onto rock surface to displace divalent ions. Nevertheless, the ammonium ion itself tends to displace more calcium ion than magnesium ion on clay surface. Adding potassium ion into ammonium ion solution results in shifting from favorability of calcium ion dissolution toward magnesium ion dissolution. Since magnesium ion creates stronger bond compared to calcium ion, ammonium ion is therefore considered to be superior to potassium ion in oil recovery mechanism. The results from imbibition and coreflooding test confirms that low salinity waterflooding in shaly-sandstone can be accomplished by the used on ammonium ion. However, ammonium ion should be prepared to favor the dissolution of calcium ion since oil that is attached through calcium ion is easier to be recovered compared to that of the dissolution of magnesium ion.

In this study, the solution of pure ammonium chloride and mixture of ammonium-calcium-sodium ion at the ratio of 40-20-40 show good potential in enhancing oil recovery. Nevertheless, the case of ammonium-calcium-sodium ion at the ratio of 40-20-40 might be suitable for the existing oilfield since sodium can be mixed with the water formulation at high portion and fresh water demand can be minimized. From the conditions tested in this experiment, oil recovery factor from the use of ammonium ion can be increased up to 26 percent.

Field of Study:	Georesources and Petroleum Engineering	Student's Signature
Academic Year:	2018	Advisor's Signature

ACKNOWLEDGEMENTS

Firstly, I would like to thank my thesis advisor, Dr. Falan Srisuriyachai, for giving me this valuable opportunity to study this interesting thesis topic. I have received several great ideas and profitable contributions throughout his advices to complete my thesis and to have a straightforward insight as a petroleum engineer. His encouragement and knowledge are the enormous motivations for me for being better in my future career.

I would like to thank to all of my thesis committees and instructors for providing knowledge in petroleum field which are really necessary for my thesis as well as my career. Additionally, I would like to thank to the Department of Mining and Petroleum Engineering for providing the laboratory and facilities.

Next, I would like to thank to the office of academic affairs, Chulalongkorn University for awarding me a full-time ASEAN scholarship. It is my honor to receive this financial support to study in a top-rank university in Thailand.

My thank goes to PTT Exploration and Production Public Company Limited for providing rock and liquid samples for this study.

I would like to thank Chevron Thailand Exploration and Production, Ltd. for financial support of this study as well as international conference fee.

I would like to send my special thanks to Mr. Ativish Yomchan, my classmate for being always supportive on experiment as well as on normal life during my stay in Bangkok.

Last but not least, I would like to dedicate this precious work to my beloved family. Thank you for being always my endless support in my life.

TABLE OF CONTENTS

	Page
ABSTRACT (THAI).....	iii
ABSTRACT (ENGLISH).....	iv
ACKNOWLEDGEMENTS	v
TABLE OF CONTENTS	vi
LIST OF TABLES	ix
LIST OF FIGURES	xi
LIST OF ABBREVIATION.....	xiii
LIST OF NOMENCLATURES	xiv
CHAPTER I INTRODUCTION.....	1
1.1 Background	1
1.2 Objectives:	3
1.3 Scope of Work	3
CHAPTER II LITERATURE REVIEW	5
2.1 Evidence of Oil Recovery by Low Salinity Waterflooding.....	5
2.2 Proposed Oil Recovery Mechanisms by Low Salinity Waterflooding	7
3.1 Salinity of Water	10
3.2 Waterflooding and Low Salinity Waterflooding	12
3.3 Ionic Properties	17
3.4 Properties of Ammonium Ion	20
CHAPTER 4 METHODOLOGY	23
4.1 Determination of Basic Parameters	23

4.1.1 Rock and Petrophysical Properties.....	23
4.1.2. Basic Properties of Brines and Crude Oil	26
4.2 Stirring Test.....	28
4.2.1 Determination of Ion Concentration by Titration.....	29
4.2.2. Determination of the Optimal Duration for Stirring Test	31
4.2.3 Determination of the Most Effective Water Formulation	32
4.3 Imbibition Test.....	35
4.4 Coreflood Test.....	36
4.5 Experimental Structure	37
CHAPTER V	40
RESULTS AND DISCUSSION.....	40
5.1 Stirring Test of NH_4^+ - Ca^{2+} - Na^+ Combination and Effects of Total Concentration	40
5.1.1 Explanation of NH_4^+ - Ca^{2+} - Na^+ Ternary Diagram	40
5.1.2 Effects of Total Concentration on NH_4^+ - Ca^{2+} - Na^+ Ternary Diagram.....	42
5.2 Stirring Test of Ammonium-Potassium-Calcium-Sodium Combination and Effects of Ammonium-Potassium Portion.....	46
5.2.1 Low Ammonium Ion Portion (Ammonium-Potassium of 1:4).....	46
5.2.2 High Ammonium Ion Portion (Ammonium-Potassium of 4:1).....	47
5.3 Imbibition Test.....	49
5.4 Coreflood Test.....	54
5.4.1 Recovery Factors.....	54
5.4.2 Ion Detections	59
CHAPTER VI CONCLUSIONS AND RECOMMENDATIONS	63

6.1 Conclusions	63
6.2 Recommendations	64
REFERENCES	65
VITA.....	69



LIST OF TABLES

	Page
Table 1 Types of water classified by salinity range as defined by total dissolved solids (TDS) in milligrams/liter (mg/L)	11
Table 2 Summary of atomic, ionic and hydrate properties of sodium ion, potassium ion and ammonium ion [21]	21
Table 3 Elemental analysis of shaly-sand samples from S1 oilfield in Thailand using XRD and XRF.....	23
Table 4 Summary of core dimensions, bulk volume, porosity, pore volume, permeability, and irreducible water saturation of rock samples.....	26
Table 5 Composition of formation water from S1 oilfield (PTTEP) based on 1 liter of solution.....	27
Table 6 Summary of fluid density and viscosity of formation water, at the concentration of 14,098 ppm, low salinity water formulations at 1,000, 2,000, 5,000 ppm and crude oil at 60°C.....	28
Table 7 Summary of total hardness of filtrate solutions obtained from different stirring times.....	32
Table 8 Volume portions of ammonium chloride, calcium chloride and ammonium chloride solutions to represent different 25 water formulations on ternary diagram.	34
Table 9 Ions compositions of formation water	50
Table 10 Ions composition of three different selected low salinity water formulations	51
Table 11 Summary of recovery factors obtained from imbibition tests of different core samples in different water formulations at different time	52
Table 12 Characteristics of core sample used in coreflooding test.....	54
Table 13 Ions component of low salinity brines in the coreflooding test.....	55

Table 14 Summary of titration test after performing coreflooding test 60



LIST OF FIGURES

	Page
Figure 1 Illustration of three different oil recovery techniques	13
Figure 2 Fractional flow curve which can be used to determine the average water saturation at breakthrough [15].....	16
Figure 3 The s-p-d-f orbital systems illustrated in red, yellow, blue and green color, respectively [19].....	18
Figure 4 Illustration of sodium ion with six molecules of water, forming hydrated structure [20]	19
Figure 5 Example of ternary diagram illustrating three apex of ammonium chloride, calcium chloride and sodium chloride solutions and 25 combinations of water formulation to cover the whole area of diagram	33
Figure 6 Schematic diagram of coreflood apparatus	37
Figure 7 Summary of stirring test and ion titrations of NH_4^+ - Ca^{2+} - Na^+ solution	39
Figure 8 Summary of the effects of potassium ion in selected NH_4^+ - Ca^{2+} - Na^+ solution.....	40
Figure 9 Summary of imbibition and coreflooding tests	41
Figure 10 Ternary phase diagrams illustrating appearance of a) calcium ion and b) magnesium ion ; c) disappearance of ammonium ion of formulation brine containing ammonium-calcium-sodium at 1,000 ppm.....	41
Figure 11 Ternary phase diagrams illustrating appearance of a) calcium ion and b) magnesium ion; c) disappearance of ammonium ion of formulation brine containing ammonium-calcium-sodium at 2,000 ppm.....	43
Figure 12 Ternary phase diagrams illustrating appearance of a) calcium ion and b) magnesium ion; c) disappearance of ammonium ion of formulation brine containing ammonium-calcium-sodium at 5,000 ppm.....	44

Figure 13 Ternary phase diagrams illustrating zones of ion activities on shaly-sandstone sample based on concentration of ammonium ion, sodium ion and calcium ion at the concentration of 1,000 ppm.....	45
Figure 14 Ternary phase diagrams illustrating appearance of a) calcium ion and b) magnesium ion; c) disappearance of ammonium ion of formulation brine containing ammonium/potassium chloride – calcium chloride – sodium chloride at 1,000 ppm.....	47
Figure 15 Ternary phase diagrams illustrating appearance of a) calcium ion and b) magnesium ion; c) disappearance of ammonium ion of formulation brine containing ammonium/potassium chloride – calcium chloride – sodium chloride at 1,000 ppm.....	48
Figure 16 Differential water saturation versus soaking time of four core samples tested with different water formulations	53
Figure 17 Oil recovery factors from coreflood tests obtained from low salinity water containing ammonium chloride at 1,000 ppm.....	56
Figure 18 Oil recovery factors from coreflood tests obtained from low salinity water containing ammonium chloride- calcium chloride – sodium chloride at ratio of 40-40-20	57
Figure 19 Oil recovery factors from coreflood tests obtained from low salinity water containing ammonium chloride- calcium chloride – sodium chloride at ratio of 40-20-40.	58
Figure 20 Illustration of dissolution mechanisms for different low salinity water formulations at 1,000 ppm.....	62

LIST OF ABBREVIATION

EOR	Enhanced Oil Recovery
CEOR	Chemical Enhanced Oil Recovery
LSWF	Low Salinity Waterflooding
MIE	Multi-component Ion Exchange
pH	potential of Hydrogen
EDTA	Ethylenediaminetetraacetic acid
TDS	Total Dissolved Salt
DLE	Double-Layers Expansion
ANFO	Ammonium nitrate/Fuel oil
XRD	X-ray Powder Diffraction
XRF	X-ray Fluorescence
ppm	part per million
PV	Pore volume
m	Meter
D	Darcy
mD	Milidarcy
cP	Centipoise
cm	Centimeter
g	Grams
ATM	Atmosphere unit
EBT	Erochrome Black T
HNB	Hydroxynaphthol Blue
psi	Pound per square inch
RF	Oil recovery factor

LIST OF NOMENCLATURES

ϕ	Porosity
q	Injection rate
A	Cross-sectional area
f_w	Fractional flow of water
k	Absolute permeability
k_{ro}	Relative permeability to oil
μ_w	Water viscosity
μ_o	Oil viscosity
P_c	Capillary Pressure
α_d	Angle of formation dip to the horizontal
k_o	Oil permeability
k_w	Water permeability
S_w	Water saturation
N_p	Oil production
ϕ_{eff}	Effective porosity
W_{dry}	Dry weight of sample
W_{sat}	Saturated weight of sample

ρ_f	Water density
S_{wi}	Irreducible water saturation



CHAPTER I

INTRODUCTION

1.1 Background

Over these years, the crude oil usage has been greatly increased around the world. A huge number of major oil producers had intended to raise the petroleum productivity in order to satisfy the worldwide oil consumption. As a result, new technology has been applied to improve the efficiency during the production life of reservoir. One of the most common techniques has been used to boost the oil accomplishment without complication and high cost is waterflooding [1]. In definition, water is injected into reservoir formation to displace oil to another adjacent production well. Nevertheless, waterflooding still has one major problem occurring when water by-passes oil due to its higher mobility compared to that of oil. This phenomenon is so called “fingering” which is known as a characteristic that highly decreases volumetric sweep efficiency. Another problem happens when water flow through reservoir layers with different permeabilities so-called multilayered reservoir. Water has tendency to flow through the layer with the higher permeability and thus, oil is left non-displaced in the lower-permeability layers. Besides, wettability also strongly affects waterflooding behavior, causing poor oil recovery when utilizing waterflooding in oil-wet system. Fortunately, Enhanced Oil Recovery (EOR) techniques were created to deal with these problems. EOR is the process to obtaining remaining oil left after primary and secondary recovery techniques through certain extraction processes. Chemical Enhanced Oil Recovery or CEOR is supposed to become one of the primary EOR techniques for light and medium oil reservoirs. This technique is performed by injecting chemicals that have abilities to improve oil recovery. These chemicals include polymer, alkali, and surfactant. However, the cost of these chemicals is still expensive and therefore, there is an attempt to find something more economical. Low Salinity Waterflooding (LSWF) and smart waterflooding are hence, the next generation techniques created. Nowadays, LSWF

has been thoroughly studied all over the world and it is considered to be a new key to maximize oil recovery. Low salinity water is defined by water with less salinity compared to that of formation water. Not only maintaining pressure of the reservoir, low salinity water also shifts rock surface equilibrium to a more water-wet condition, resulting in reduction of residual oil. Injection of low salinity water has widely been practiced due to availability of water sources and the technique is relatively cheaper than other techniques. Apparently, people believe that LSWF could provide higher oil recovery [2]. Theoretically, implementation of LSWF provides both physical and chemical displacements of oil, raising higher potential compared to conventional waterflooding where salinity of injected water is not considered. Dissolution of ion-binding between negative-charged sandstone surface and carboxylic compounds in crude oil together combined with replacement of monovalent ions such as sodium and potassium ions in brine are explained for oil recovery mechanism [3]. Surprisingly, Ammonium ion comes out as a perfect alternative chemical in multi-component ion exchange mechanism due to its suitable physical and chemical properties as well as its less effect to environment together with its reasonable cost.

Ammonium ion is a very common ion in petroleum industry as it is used to control disaggregation of sand grains and clay controls [4]. Therefore, ammonium can be used in conjunction with LSWF, to obtain the highest benefits in oil production. In this study, evaluation of LSWF using ammonium ion and the necessary conditions in shaly-sandstone reservoir is performed. Shaly-sandstone sample from S1 oilfield (PTTEP) located in the north of Thailand is used to represent reservoir rock. The study is commenced with stirring test using grinded rock sample and ammonium solution. Disappearance of ammonium ion and appearance of divalent ions by color titration ensure the Multi-component Ion Exchange (MIE) mechanism. Interference of other presented ions in make-up water is also studied. The interest ions include sodium ion, calcium ion and potassium ion. Interference of ion more than two species will be illustrated on ternary phase diagram. Selected formulation of LSWF containing ammonium ion will be tested for imbibition rate. The last step of study is confirmed by displacement mechanism in coreflood apparatus. The increment of oil

recovery is detected when injected water is switched from formation water to LSWF with ammonium ion [5]. Appearance of divalent ions and disappearance of ammonium ion are utilized as major criteria in this study. Together with oil recovery obtained from imbibition and coreflood tests, the best low salinity water formulation is identified.

1.2 Objectives:

First, effectiveness of ammonium ion in low salinity water during low salinity waterflooding in shaly-sandstone formation is evaluated. Moreover, certain conditions for implementation of low salinity waterflooding with ammonium ion in shaly-sandstone formation, emphasizing on interference of other potential ions are identified.

1.3 Scope of Work

This study aims to evaluate the effectiveness of ammonium ion in low salinity waterflooding when applied in shaly-sand reservoir. Complexometric titration is selected as a main method to determine the amount of divalent ion released from the MIE mechanism whereas disappearance of ammonium ion is performed by back titration with hydrochloric acid. Imbibition test and coreflood tests are designed to evaluate magnitude of change in oil recovery from conventional waterflooding to LSWF with ammonium ion. The constituent of injected low salinity water including sodium ion, calcium ion and ammonium ion are arranged in different ratios to determine the formulation where the highest liberation of divalent ion together with the highest consumption of ammonium ion is observed through ternary diagram. For three-component study, total salinity is kept constant at three different values. After that, the apex of ammonium ion is replaced by the combination of ammonium and potassium ions. As potassium is similar in terms of hydration to ammonium ion, a mixture of ammonium and potassium ions is tested to assess different benefits of each ion. Two ammonium-potassium ion formulations are tested. Selected

formulations based on the best MIE mechanism is used for imbibition and coreflood for confirmation of MIE that is believed to be responsible for oil recovery mechanism.



CHAPTER II

LITERATURE REVIEW

In this section, relevant researches are summarized. Due to many published papers related to LSWF in last decades, papers are grouped into two categories: the first group summarizes previous studies showing evidence of oil recovery by means of LSWF, whereas the second group of studies proposes oil recovery mechanisms by LSWF.

2.1 Evidence of Oil Recovery by Low Salinity Waterflooding

Tang and Morrow observed that the increase in oil recovery was obtained with a decrease in salinity by tracking the result from cyclic waterflooding [6]. Adsorption from crude oil, the presence of potentially mobile fines and the initial water saturation are all necessary conditions for an increase in oil recovery with a decrease in salinity. A presence of mobile fines occurs when clays lose their stabilities by heating or extensive flooding, and it is greatly reduced for rock with low clay content. Furthermore, clays must initially reside in connate water because if core is saturated with crude oil first, the sensitivity will be eliminated. In waterflooding, crude oil can be adhered to fine particles in different two ways: (1) crude oil can remain as drops adhering to fine particles at the pore walls as part of the trapped oil fraction, and residual crude oil can be associated with patches of kaolinite; (2) the mixed-wet clay particles are swept away from pore walls along with the oil flow and try to stick at the oil-water interface. Productions of fine particles, change in pH value and increase in pressure drop after injecting water at a constant rate, were observed. After establishing residual oil saturation by waterflooding, the crude oil recovery rate at high water-cut could be curtailed according to the composition of the injected water. Besides, heavy polar components of crude oil are adsorbed onto particles at pore walls to generate mixed-wet fines. Differences in oil

recovery with salinity can be said to be the effects of brine chemistry on the forces required to sweep these particles from the pore surface during the waterflooding.

Jie Yang et al. confirmed the influence of cations and ionic strength of initial water on primary wettability and the decrease of salinity of injected brine on wettability alteration by performing spontaneous imbibition experiments to macroscopic study [7]. The results showed that divalent ion (calcium ion) of initial water can significantly shift the initial wetting phase to be more oil-wet, meanwhile the primary wetting status does not depend on the concentration of sodium ion. The higher the concentration of calcium ions, the more oil-wet condition the core plug is. It can be explained that rising salinity of the thin film of water between oil and minerals leads to less negatively charged brine-rock and brine-oil interfaces, and as a result, the electrostatic repulsive forces of oil and rock is broken. Then, the calcium bridges are much stronger than sodium bridges. So, the rock surface was overlaid by the hydrocarbon layers, made them more oil-wet. Besides, reducing the ionic strength of imbibing water can improve the oil recovery, the explanation was because of the existence of less cations between the acid group and mineral surface with the reduction of salinity, leading to the desorption of acidic contaminants from the rock surface. As a result, adsorbed residual oil was released.

Srisuriyachai et al. believed that potassium ion was more effective ion than sodium ion in replacing divalent ions and the presence of only small amount of potassium ion was sufficient for spontaneous imbibition as it can be balanced by other potential ions [3]. Waterflooding technique was performed to observe the amount of oil recovery, whereas the imbibition test of core sample and detection of ions in effluent by ETDA were performed to measure concentration of calcium ion released from rock surface after low salinity waterflooding. Potassium ion forms its hydrated structure with a few numbers of water molecules around, causing small hydrated size, whereas sodium ion forms larger hydrated structure due to more hydration number. As a result, potassium ion is greater in term of mobility and reactivity compared with sodium ion in spontaneous imbibition. Moreover, performance of low salinity water was highly dependent on the concentration of potassium because higher number of molecules to replace divalent ion resulted in

higher possibility of replacement. Nevertheless, not only monovalent ion was required in the mechanism, the combination of others ion was also a key factor for low salinity waterflooding. Calcium ion was also found to be responsible for aiding potassium ion. With the coincident of preventing clay problems, potassium chloride proved to be an effective chemical in LSWF especially in shaly-sand formation.

2.2 Proposed Oil Recovery Mechanisms by Low Salinity Waterflooding

AlQuraishi et al. focused on the recovery oil mechanisms from LSWF in both secondary and tertiary modes [8]. All in all, LSWF was the method that has a good potential for sandstone and carbonate formations in both production modes that highly increases the amount of oil recovery. In fact, the wettability alteration plays an important role for improving oil recovery, including contact angle and zeta potential. Diluting of seawater by ten times could shift the intermediate-wet rock to water-wet rock, meaning that oil attached on rock surface was liberated and replaced by water. On the other hand, zeta potential also determined the wettability alteration: the value of zeta potential was lower in the case of 10-time diluted seawater. This led the positive charges on rock surface turning into negative charges, releasing the attached oil. Another conclusion was that multi-component ions exchange occurred during the LSWF, coming along with the anhydrite dissolution, explaining the enhanced oil recovery in the sandstone samples. The recovery mechanism, in addition, referred to fine migrations and detachment of mixed-wet kaolinite clay particles. During the test, fine production was observed and a small percentage of residual oil was recovered and it was believed to attribute to the incremental of oil recovery by stepwise LSWF. Moreover, the initial rock wetting condition was also a critical indicator concerned when it came to the potential of LSWF; if the rock itself had lower irreducible water saturation, the secondary mode with high salinity could be more effective than the tertiary mode by water with lower salinity. Finally, the drop of interfacial tension by salinity reduction did not have contribution to an oil recovery.

Srisuriyachai and Muchalintamolee studied the effects of total salinity and ratio of calcium and magnesium ion on effectiveness of LSWF by observing displacement by water ratio which is part of measurement of wettability index [9]. The dominant of foreign ions or decreasing of calcium ion and magnesium ion could change the equilibrium of rock fluid system, leading to MIE mechanism. The difference between high salinity formation water and injected low salinity water determined the value of displacement by water ratio. Results showed that higher difference in salinity between formation and injected water corresponded to higher displacement by water ratio. This could be explained by the dissolution of bridging divalent ion through MIE mechanism. Another conclusion was that the amount of calcium ion in the injection water was required; however, too small amount of calcium ion was not adequate to trigger the MIE process. On the other hand, too high calcium ion concentration resulted in lowering of displacement by water ratio due to obstruction of dissolution of calcium ion. Therefore, concentration of calcium ion in injected water should be kept moderately, as well as ratio of calcium ion to magnesium ion should be equal to overcome interference from magnesium ion that could inhibit dissolution mechanism.

Pu et al. discovered the concept that dissolution of anhydrite cement in sandstone formation was one of the main mechanisms besides MIE without the presence of clay, by conducting the waterflooding tests and spontaneous imbibition tests [10]. The liberation of fine embedded minerals which are likely to be associated with dissolution of anhydrite from the cement could be major reason for the observed response from LSWF. The flooding of sandstone core with sodium chloride solution resulted in an increase in concentration of sulfate ions instead of calcium ions. This could be explained that the core was not shaly-sand but it was nearly pure sandstone. Then, the only possible mechanism for enhance oil recovery was the replacement of cement components by divalent ions in low salinity water. On top of that, the movement of cement components could contribute a possible factor in a wide range of observed relationship between oil recovery and pressure decrease. The difference in behavior of cores from the oil and the water zone suggested that enhanced oil recovery by LSWF turned the wetting condition from mildly water-wet

towards moderately water-wet by a mechanism involving dissolution of anhydrite associated with releasing of other fine materials from pore space.

From all chosen literatures, it is obvious that LSWF is one of the EOR methods which can be effectively implemented to most oilfields. However, these research works only mentioned the effectiveness of water containing presented ions in formation water or seawater. As ammonium ion which is a foreign monovalent ion that possesses similar characteristic to potassium ion; it should have therefore, capacity in creating MIE mechanism as well as increase oil recovery.



CHAPTER III

RELEVANT THEORY

3.1 Salinity of Water

Salinity is the amount of salt dissolved in a body of water which is measured in grams of salt over kilograms of seawater [11]. Salts are compounds like sodium chloride, magnesium sulfate, potassium nitrate, and sodium bicarbonate which dissociate into ions when dissolve in water. Salinity is a measure of all the salts dissolved in water. Salinity is usually measured in grams/kilograms. Seawater typically has salinity of around 35 g/kg, although lower values are typically observed near coastlines where rivers enter to the seas. This means that in every kilogram (1,000 grams) of seawater, 35 grams are salt. Rivers and lakes can have a wide range of salinities, from less than 0.01 g/kg to a few g/kg, although there are many places where higher salinities are found. Because the water in estuaries is a mix of fresh water and ocean water, the salinity in most estuaries is less than the open ocean. Bottom water almost always contains more salt than surface waters.

The salt in the ocean is mostly made up of the elements sodium (Na) and chlorine (Cl). Together they account for 85.7% of the dissolved salt. The other major components in seawater are magnesium (Mg), calcium (Ca), potassium (K) and sulfate (SO₄). Together with chlorine and sodium, they make up 99.4% of the salt in the ocean.

The term 'salinity' is, for oceanographers, usually associated with one of a set of specific measurement techniques. As the dominant techniques evolve, so do different descriptions of salinity. Salinities were largely measured using titration-based techniques before the 1980s. Titration with silver nitrate could be used to determine the concentration of halide ions (mainly chloride and bromide) to give a chlorinity. The chlorinity was then multiplied by a factor to account for all other constituents.

During the reservoir generation, water occupied pore space first in sedimentary rock, which is so-called formation water, can flow under the

hydrodynamic condition. Otherwise, if the formation water is already trapped in pores at the beginning of deposition and unable to liberate out, it is known as connate water. These kinds of water contain dissolved salts at a significant level due to their natural origin. According to Carpenter classification of salted water, brine have to contain at least 100,000 mg/L total dissolved salts, saline water containing from 10,000 to 100,000 mg/L and fresh water containing less than 10,000 mg/L. Seawater is also classified as saline water, because its average salinity is 35,000 mg/L [12] Table 1 summarizes ranges of total solid dissolves of different types of water with their remarks.

Table 1 Types of water classified by salinity range as defined by total dissolved solids (TDS) in milligrams/liter (mg/L)

Water type	Total Dissolved Solids (TDS) in Milligrams/Liter	Comment
Fresh	Less than 500	Typical fresh range
Saline	1,000 to 10,000	Seawater is ~35,000
Brine	35,000 to 200,000	
Oil and Gas co-produced water	~500 to over 200,00	Derived from oil and gas production
Fully salt saturated	Greater than 250,000	Found in some oil and gas produced waters and deep saline reservoirs

Compositions and characteristics of formation water come from a combination of various factors such as depositional environment, formation mineralogy, historical parameters including temperature and pressure. Therefore,

different subsurface reservoirs generate different compositions and properties of formation water.

Despite of the wide range in nature of formation water around the world, they still had a same tendency. For instance, calcium ion and chloride ion are enriched in formation water, but impoverished in sodium ion, sulfate ion and potassium ion compared to seawater. Chloride ion is making up to 94% by total mass of anions in sedimentary formation water, turning it into the most remarkable anion in oilfield brines. Water with salinity less than 10,000 mg/L may contain sulfate ion or bicarbonate ion. Oilfield water generally contains more sodium ion by weight than other cations, but during evaporation, most of sodium content of brines increases when halite precipitated. As a result, calcium ions are enriched and turn to be the most dominant cations in terms of mass. Potassium ion exists as another dominant ion in many reservoir fluids but until present only a small amount showed up.

The composition of formation water in carbonate and sandstone formation is generally different. Sulfate is the most active ion regarding wetting properties in carbonate formation and due to the high concentration of calcium ion in the formation brine under the high temperature condition; they could precipitate into anhydrite (CaSO_4). The presence of sulfate in the formation water will increase the water-wet condition of the system. On the other hand, sandstone formation composes of many different minerals including sodium ion, potassium ion, magnesium ion, calcium ion and hydrogen ion which can be adsorbed onto the clay surface. These cations, especially calcium ion and hydrogen ion, are significantly necessary in the oil recovery mechanism by means of LSWF [13].

3.2 Waterflooding and Low Salinity Waterflooding

Waterflooding is known as oil recovery technique implemented by injecting water to increase production from oil reservoirs. The use of water to increase oil production is known as "secondary recovery" and it is typically performed after "primary recovery," which uses the natural energy of reservoir itself (fluid and rock

expansions, solution-gas drive, gravity drainage, and water influx) to produce oil. Figure 1 illustrates a summary of oil recovery techniques including primary recovery, secondary recover and also tertiary recovery which is so-called Enhanced Oil Recovery or EOR (generally considered as a phase beyond waterflooding). Water is injected to support pressure of the reservoir (also known as a voidage replacement), and also to sweep or displace oil from the reservoir, pushing it towards a production well. Sources of water can be seawater, aquifer water, water from river, and also produced water.

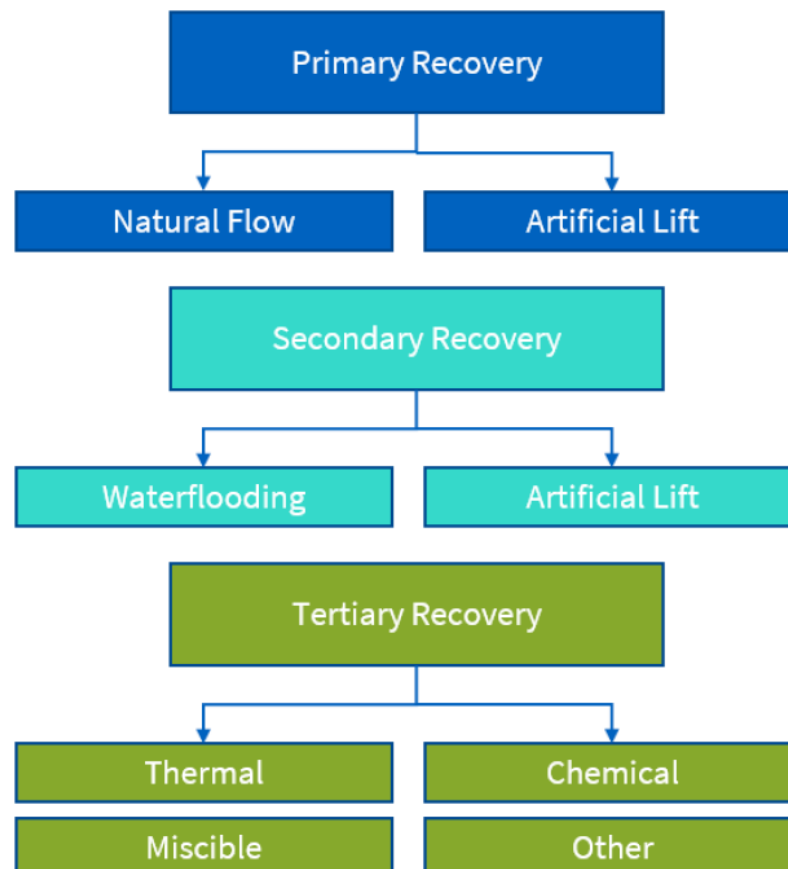


Figure 1 Illustration of three different oil recovery techniques

The major purpose of waterflooding is to increase oil production rate and, ultimately, the total oil recovery. This is accomplished by "voidage replacement"—injection of water to increase reservoir pressure to its initial level and maintain it at that pressure as long as possible. Injected water displaces oil from pore spaces, but

the efficiency of such displacement depends on many factors such as oil viscosity and rock characteristics. To understand the reservoir rocks, petroleum engineers must consider the depositional environment at the pore and the reservoir levels as well as other possibilities at several levels in between. Diagenetic history of reservoir rocks must be ascertained. Structure and faulting of the reservoir must be determined, understanding the inter-connectivity among all parts of the reservoir. Besides, water-oil-rock characteristic need to be well understood because they control wettability, residual oil saturation to waterflood and relative permeability to oil at higher water saturation.

The level of effectiveness of waterflooding depends on mobility ratio between the oil and water, and geology of oil reservoir. Waterflooding is effective because most reservoir rocks are either water-wet or mixed-wet. The depositional and diagenetic characteristics of a reservoir control major aspects of the water-oil displacement process. These characteristics can either enhance waterflood performance or have detrimental effects on the water-oil ratio as a function of time. Often, the details of reservoir geology are not known until production wells start producing injected water.

One of the simplest and most widely use methods of estimating the advance of a fluid displacement front in an immiscible displacement process is the Buckley-Leverett method. The Buckley-Leverett theory estimates the rate at which an injected water front moves through porous medium based on five assumptions: 1) flow is vertical or horizontal; 2) water is injected into an oil reservoir; 3) oil and water are both incompressible; 4) oil and water are immiscible; and 5) gravity force and capillary pressure maybe be neglected in some certain cases [14].

According to Buckley-Leverett problem, the continuity equation for water is written as:

$$\frac{\partial S_w}{\partial t} + \frac{q}{A\phi} \frac{df_w}{dS_w} \frac{\partial S_w}{\partial x} = 0 \quad (\text{Equation 1}),$$

where q is injection rate, A is the cross-sectional area, and ϕ is porosity.

Characteristics of waterflooding can be presented by fractional flow equations. The fractional flow of water, f_w is according to the paper of Leverett published in 1941, derived from Darcy's Law for oil and water:

$$f_w = \frac{1 + \frac{k \cdot k_{ro}}{v_t \cdot \mu_o} \left[\left(\frac{\partial P_c}{\partial L} \right) \right] - g \Delta \sin \alpha_d}{1 + \frac{\mu_w k_o}{\mu_o k_w}} \quad (\text{Equation 2}),$$

where k is absolute permeability, k_{ro} is relative permeability to oil, and μ_w and μ_o are water and oil viscosities, P_c is capillary pressure, α_d is angle of formation dip to the horizontal.

The above equation depends on three main factors: capillary pressure, gravity force and viscous force. However, the capillary pressure term is neglected in practical use because of its insignificant value compared to viscous force and gravity force, so that vertical flow equation can be modified as:

$$f_w = \frac{1 + \frac{k \cdot k_{ro}}{v_t \cdot \mu_o} (g \Delta \sin \alpha_d)}{1 + \frac{\mu_w k_o}{\mu_o k_w}} \quad (\text{Equation 3}).$$

To illustrate the general use of fractional flow curve, flow in horizontal direction is explained. Even further simplification can be done where the displacement happens in a horizontal system, then the gravity force and capillary forces can be both neglected, the equation can be abbreviated to:

$$f_w = \frac{1}{1 + \frac{\mu_w k_o}{\mu_o k_w}} \quad (\text{Equation 4}).$$

Using known relative permeability curves for both oil and water, and fluid viscosities, fractional flow curve can be constructed as a function of water saturation as illustrated in figure 2.

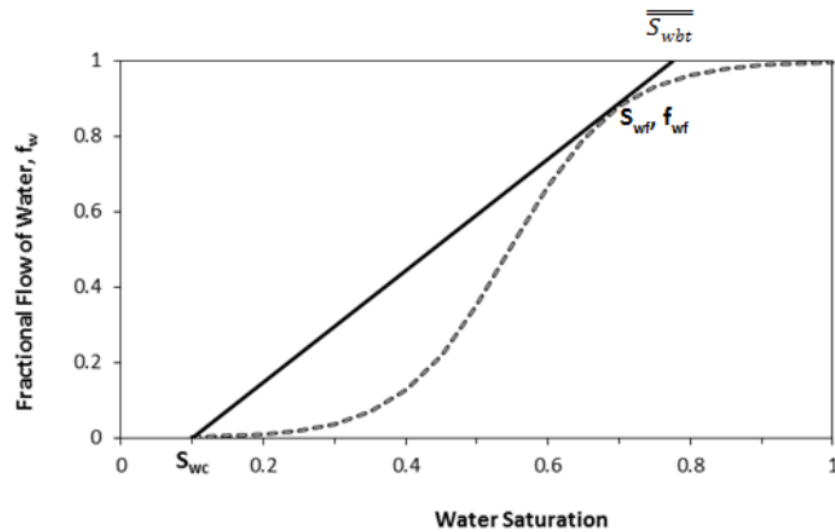


Figure 2 Fractional flow curve which can be used to determine the average water saturation at breakthrough [15]

After water breakthrough, the Welge integration gives the oil recovery in place, N_p , implicitly as:

$$N_p = \frac{S_w - S_{wir} + (1 - f_w)t_D}{1 - S_{wir}}, \text{ for } t_D > t_{D1} \quad (\text{Equation 5}).$$

At $t_D = 1/f_w'(S_{w1})$ and t_D must be greater than t_{D1} and before breakthrough, N_p is simply calculated by:

$$N_p = \frac{t_p}{1 - S_w}, \text{ for } t_D \leq t_{D1} \quad (\text{Equation 6}).$$

Conventional fractional flow theories such as the Buckley-Leverett analysis have contributed to the benefit for reservoir engineers throughout many years. Despite of its simplicity, these analyses provide decent estimations of water breakthrough and oil bank height/duration in the experiments and the fields.

Low Salinity Waterflooding (LSWF) is an emerging EOR technique in which chemistry plays major role in improving oil recovery and the method uses water with a low concentration of dissolved salts as a flooding medium. Sources of low salinity water are typically rivers, lakes or aquifers associated with meteoric water. There are several mechanisms which have been approved scientifically including fine migration,

pH rising, Multi-Ion Exchange (MIE) and Double-Layers Expansion (DLE) [16]. MIE from time to time has proved to be an important mechanism in LSWF. It can be explained when abundant of foreign ion or the reduction of calcium and magnesium ions changes equilibrium of rock-fluids system, and easily be replaced by monovalent ion such as sodium ion or potassium ion. During the injection of low salinity water, MIE will take place, removing polar compounds and organo-metallic complexes from the surface and replacing them with un-complex cations, from then enhancing oil recovery. Besides, the movement of fine materials in sandstone is also a factor to concern about. This mechanism occurs when ionic strength of injected water is less than a critical flocculation concentration which strongly depends on the relative concentration of divalent ions. The clay and silt dispersing in water can clog the smaller pores or pore throats, then formation permeability is reduced, leading to increment of sweep efficiency when water has to flow through another flow paths. Ion exchange between adsorbed Na^+ and H^+ in solution in low salinity injected water leads to a boost of OH^- concentration in bulk solution, rising pH value. The permeability will slightly change when pH value of fluids increasing until 9, and at pH higher than 11 a drastic decrease in the permeability was observed [17].

3.3 Ionic Properties

Ions are defined as particles that carry electrical charges. Condensed phases, solids and liquids, are electrically neutral; that is, ions compose of positively and negatively charged particles – cations and anions, respectively – that may be bound or relatively free to migrate. An electrolyte is a neutral combination of cations and anions that can exist as a chemical substance capable of dissociating into its constituent ions in a suitable environment, like aqueous solution. Ions may be monatomic (such as Na^+ or Br^-), may consist of a few atoms (such as NH_4^+ or SO_4^{2-}), or be much larger, consisting of many atoms. Isolated ions may be regarded as existing in an ideal gaseous state that is without interactions with other particles or their surroundings in general. Some large ions are produced in mass spectrometers, but commonly isolated ions consist of relatively few atoms. They may, however, be

the centers of clusters consisting of the ion proper surrounded by a small number of solvent molecules.

An atom is a basic unit of an element. The identity of an element is determined by number of positively charged protons in the atomic nucleus. A stable atom contains the same number of electrons as protons and no net charge. When electrons are added or removed, the stable atom becomes an ion. If electrons are removed, the net charge of the ion will be positive and known as a cation. When electrons are added, the net charge of the ion becomes negative and known as an anion.



An atomic orbital is a mathematical function that describes the wave-like behavior of either one electron or a pair of electrons in an atom. This function can be used to calculate the probability of finding any electron of an atom in any specific region around the atomic nucleus. Each orbital in an atom is characterized by a unique set of values of the three quantum numbers: n , l , and m , which respectively correspond to the electron energy, angular momentum, and an angular momentum vector component (the magnetic quantum number). Each such orbital can be occupied by a maximum of two electrons, each with its own spin quantum number s . The simple names s orbital, p orbital, d orbital and f orbital refer to orbitals with angular momentum quantum number $l = 0, 1, 2$ and 3 respectively [18]. Figure 3 depicts possible orientations of s - p - d - f orbital systems in three dimensions.

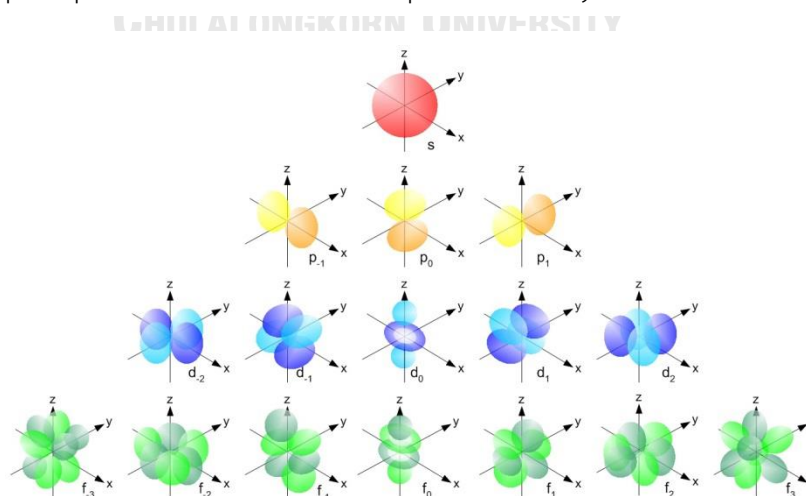


Figure 3 The s - p - d - f orbital systems illustrated in red, yellow, blue and green color, respectively [19]

Aqueous ion, which is the ion in aqueous solution, dissolved in water, of chemical formula $[M(H_2O)_n]^{z+}$. The solvation number, n , determined by a variety of experimental methods is 4 for Li^+ and Be^{2+} and 6 for elements in periods 3 and 4 of the periodic table. Lanthanide and actinide aqua ions have a solvation number of 8 or 9. The strength of the bonds between the metal ion and water molecules in the primary solvation shell increases with the electrical charge, z , on the metal ion and decreases as its radius, r , and increases. The water molecules directly attached to the metal ion are said to belong to the first coordination sphere, also known as the first, or primary, solvation shell. The bond between a water molecule and the metal ion is a dative covalent bond, with the oxygen atom donating both electrons to the bond. Figure 4 shows the aqueous ion $[Na(H_2O)_6]$, the oxygen atoms are arranged at the vertices of a regular octahedron centered on the sodium ion.

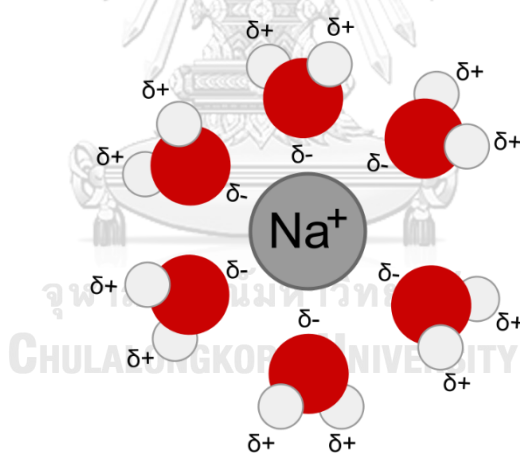


Figure 4 Illustration of sodium ion with six molecules of water, forming hydrated structure [20]

Mobility of molecules is affected by the size, charge, shape of an ion and solvent composition. The effects of ion-size, ion-charge and ion-shape cumulatively define the charge density. Very small ions, regardless of charge, have very high charge density and so are solvated to a large extent in water or other highly polar solvents. Extensive solvation effectively increases the size of small ions. Very large

ions are usually limited by their physical size to slow movement. Intermediately sized ions are generally most mobility.

3.4 Properties of Ammonium Ion

The ammonium cation is a non-metal ion which is positively charged polyatomic ion with the chemical formula NH_4^+ . It is formed by the protonation of ammonia (NH_3). Ammonium is also a general name for positively charged or protonated substituted amines and quaternary ammonium cations (NR_4^+), where one or more hydrogen atoms are replaced by organic groups.

The ammonium ion is generated when ammonia, a weak base, reacts with Brønsted acids (proton donors):



The ammonium ion is mildly acidic, reacting with Brønsted bases to return to the uncharged ammonia molecule:



Thus, treatment of concentrated solutions of ammonium salts with strong base gives ammonia. When ammonia is dissolved in water, a tiny amount of it converts to ammonium ions:



The degree to which ammonia forms the ammonium ion depends on the pH value of the solution. If the pH value is low, the equilibrium shifts to the right: more ammonia molecules are converted into ammonium ions. If the pH value is high (the concentration of hydrogen ions is low), the equilibrium shifts to the left: the hydroxide ion abstracts a proton from the ammonium ion, generating ammonia.

Despite of the fact that ammonium ion could not be found in formation water as well as seawater, it is still considered to replace divalent ions during MIE mechanism when comparing to sodium ion and potassium ion. Ammonium ion has no atomic number since it is made up of two different atoms, while sodium atomic number is 11 and potassium atomic number is 19. The ionic diameter in aqueous condition of sodium ion is 3.6 Å, meanwhile these parameters of potassium and ammonium ions are 3.3 Å. These ions are different when they combined with the water clusters surround them. In common, sodium ion is enclosed by 5 to 11 molecules of water, while the number of water clusters surrounding potassium ion and ammonium ion is around 1 to 4 molecules. This leads to the consequences that hydrated sodium is larger in size compared to potassium ion and ammonium ion. Despite of larger atomic radii, the mobility of ammonium ion is still faster than sodium ion for its mobility. Table 2 summarizes properties of sodium, potassium and ammonium ion.

Table 2 Summary of atomic, ionic and hydrate properties of sodium ion, potassium ion and ammonium ion [21]

Ion	Atomic Number	Ionic radius (pm)	Hydration Number	Hydrated radius (Å)	Ionic mobility ($10^8 \text{ m}^2 \text{ s}^{-1} \text{ V}^{-1}$)
Sodium	11	116	5-11	3.6	5.62
Potassium	19	152	1-4	3.3	7.62
Ammonium	-	175	1-4	3.3	7.62

Because of small amount of water molecules surrounding in hydrated system, ammonium ion can be utilized as clay control agent. The diameter of cations is in relation to the size of opening toward tetrahedral clay structure, which is between 2-3 angstroms in width and depth. Therefore, ammonium ion size is quite similar to the size of opening sheet of clay units and as a consequence, ammonium ion can be

used to maintain the charge stability and structural stability of the opening sheet of clays [22].

Ammonium ion contributes a large amount of application in the industry. Ammonium nitrate is an important fertilizer with the N-P-K rating 34-0-0 (34% nitrogen). Ammonium nitrate readily forms explosive mixtures with varying properties when combined with primary explosives such as azides or with fuels such as aluminum powder or fuel oil. ANFO is a mixture of 94% ammonium nitrate ("AN") and 6% fuel oil ("FO") widely used as a bulk industrial explosive. It is used in coal mining, quarrying, metal mining, and civil construction in undemanding applications where the advantages of ANFO's low cost and ease of use matter more than the benefits offered by conventional industrial explosives, such as water resistance, oxygen balance, high detonation velocity, and performance in small diameters.



CHAPTER 4

METHODOLOGY

The study is divided into four major parts, including the evaluation of basic parameters, stirring test, imbibition test, and coreflooding test. The optimal water formulation is chosen based on appearance of divalent ions that are released during MIE mechanism together with disappearance of monovalent ion that is believed to displace the sites of divalent ions. Appearance and disappearance of ions are performed by color titration of filtrate from stirring test or effluent from coreflood test.

4.1 Determination of Basic Parameters

4.1.1 Rock and Petrophysical Properties

Rock sample in this study was taken from S1 field of PTTEP located in the north of Thailand. Lithologically, the rock is shaly-sandstone with high content of shale. Table 3 summarizes elemental analysis from XRD and XRF. From the table, it can be seen that after silicon and aluminium, the rock contains high portion iron, potassium and magnesium ions and these are ions that are bound with clay component.

Table 3 Elemental analysis of shaly-sand samples from S1 oilfield in Thailand using XRD and XRF

Elements	Si	Al	Fe	K	Mg	Ti	Ca	P	Cl
%	27.154	5.766	3.001	1.842	0.697	0.661	0.292	0.281	0.174
Elements	Na	S	Zr	Mn	Sn	Cr	Vi	Zn	Ni
ppm	488.3	485.3	399.7	357.3	278.8	137.5	118.6	91.6	59.9

Rock samples used in this study were divided into two groups: the first was grinded sample used for stirring test; and the second group which was core sample utilized for imbibition and coreflood tests. For grinded sample, it can be grinded from both cuttings and core samples. First, grinded rock was used to measure for grain density. The value of about 2.52-2.56 g/cm³ dictates that rock sample contains quite high portion of shale making the grain density to be much differ from 2.65 g/cm³ for the case of pure sandstone. Based on the clay content report obtained from PTTEP, majorities of clay found in this field are illite, kaolinite and monmorillonite. In certain location the shale volume can be reached up to 60 percent.

Most rock properties were measured on core samples. In this study, four core samples were utilized. Prior to the use of core samples, cores must be cleaned by solvent extraction or so-called SOXHLET extraction. Each sample was cleaned by toluene reflux for 24 hours followed by another 24 hours by methanol. Toluene was mainly functioned to remove heavy hydrocarbon, whereas methanol removed light hydrocarbon, residual water and also remaining toluene from the previous step. Clean samples were rested in oven at the temperature of 70°C to remove humidity and were stored in desiccator prior to the saturation process. Important rock and petrophysical properties in this study are effective porosity, absolute permeability, and irreducible oil saturation.

For effective porosity, samples were fully saturated by coreflood machine using formation water to avoid the problems of clay migration and clay swelling which are common concerns for shaly-sandstone. The information of preparation of formation water is in section 4.1.2. Effective porosity is simply performed by measured dry weight, saturated weight, core dimensions and density of formation water. Equation 4.1 shows how to obtain the effective porosity of core sample:

$$\varphi_{eff} = \frac{W_{sat} - W_{dry}}{\rho_f} \quad (\text{Equation 10}),$$

where φ_{eff} is effective porosity, W_{dry} is dry weight of sample in grams, W_{sat} is saturated weight of sample in grams, and ρ_f is water density in g/cm³.

From equation 4.1, the measurement of fluid density is explained in section 4.1.2. Once porosity is known, a more important parameter can be obtained which is pore volume (PV). Pore volume is simply obtained by multiplying calculated bulk volume by the porosity obtained from equation 4.1. As core sample is in the cylindrical shape, diameter and length of core sample is required for calculation. Measurement of core dimension is performed by using Vernier calliper.

For absolute permeability (k_a), a fully-saturated sample is placed in coreflood apparatus again and formation water is used as flowing fluid. As coreflood apparatus can control fluid injection at the constant rate, different pressure across the core sample can be detected during the steady-state flow where volume of entering fluid is equal to volume of exiting fluid. Absolute permeability can be calculated from:

$$k_a = \frac{q\mu L}{A\Delta P} \quad (\text{Equation 11}),$$

where k_a is absolute permeability (Darcy), q is injection rate (cm^3/sec), μ is viscosity of the saturated fluid (cP), L is length of the core sample (cm), A is cross-sectional area of the core sample (cm^2), and ΔP is differential pressure across the core sample (ATM).

Once core sample is fully saturated and porosity, pore volume and absolute permeability are measured, samples are followed by the displacement by oil to imitate the oil migration process. Heated oil above its pour point is injected through core sample using coreflood apparatus until no more formation water was being displaced and detected at the producing end. Total amount of produced water is collected and subtracted by dead pore volume of the coreflood system. This volume represents part of the coreflood that is responsible for the liquid volume at the producing end but it is not the volume that comes from pore volume. Volume of water with dead volume is therefore, the volume that oil occupies in core sample and the difference between pore volume and volume of oil in core sample determines irreducible water. At this step, irreducible water saturation (S_{wi}) can be calculated from:

$$S_{wi} = \frac{V_p - V_w}{V_p} \quad (\text{Equation 12}),$$

where S_{wi} is irreducible water saturation (fraction), V_p is pore volume (cm^3) and V_w is volume water recovered after oil flood and subtracted by dead pore volume of the machine (cm^3). Table 4 summarizes physical and petrophysical properties including diameter, length, bulk volume, porosity, pore volume, permeability, and irreducible water saturation of rock samples used in this study. After core samples attain their initial water saturation, cores are soaked in crude oil and aged for a period of two weeks to allow the completion of wettability equilibrium.

Table 4 Summary of core dimensions, bulk volume, porosity, pore volume, permeability, and irreducible water saturation of rock samples

Sample	Radius (cm)	Length (cm)	Bulk Volume (cm^3)	Dry weight (g)	Permeability (mD)	Porosity	Pore volume (cm^3)	IWS
44	3.79	8.14	91.872	189.74	181.02	0.194	17.87	0.449
19	3.79	8.57	96.726	205	74.28	0.180	17.49	0.681
17	3.76	8.18	90.868	195.6	52.91	0.167	15.21	0.490
25	3.77	8.2	91.575	202.82	25.11	0.145	13.28	0.432

CHULALONGKORN UNIVERSITY

4.1.2. Basic Properties of Brines and Crude Oil

In this study, fluids used are mainly formation water, injected water and crude oil. Important properties of each fluid are described separately in each subsection.

For formation water, water is prepared based on the ionic composition obtained from S1 oilfield. From cationic and anionic balance, formation water at the concentration of 14,098 ppm can be prepared from sodium chloride (NaCl), potassium chloride (KCl), magnesium chloride (MgCl_2), Calcium Chloride (CaCl_2) and

sodium hydrogen carbonate (NaHCO_3). Table 5 summarizes composition of formation water from S1 oilfield based on each preparing chemical.

Table 5 Composition of formation water from S1 oilfield (PTTEP) based on 1 liter of solution

Chemical	MW	Weight (g)
NaCl	58.5	12.403
KCl	74.6	0.160
MgCl_2	95.0	0.110
CaCl_2	111.0	0.706
NaHCO_3	84.0	0.719
Total		14.098
Total Dissolved Solid = 14,098 ppm		

Two important properties of formation water required for this study are fluid density and fluid viscosity. As mentioned in equation 4.1 and 4.2, fluid density and fluid viscosity are required for the calculation of effective porosity and absolute permeability. Fluid density is simply measured by using pycnometer with the known exact volume. The difference weight of empty pycnometer and pycnometer filled up with formation water results in acquiring of both fluid weight and fluid volume and eventually, fluid density can be determined. For fluid viscosity, the measurement is performed by using Cannon-Fenske viscometer where the speed of fluid flowing through the capillary tube together fluid density determines fluid viscosity in centipoise. As the testing temperature can be both at room temperature (around 30°C) and elevated temperature close to reservoir temperature (60°C), density and viscosity of formation brines are measured at both temperatures.

The injected brine in this study is water containing less amount of salt compared to formation water. The chosen concentrations of injected brine are in the range from 1,000 to 5,000 ppm. The only importance property of injected brine is

this study is the fluid density as it is importance for calculation of fluid saturation during imbibition test (section 4.3). Similarly, density of crude oil should be provided to complete this calculation. Hence the imbibition test must be conducted at elevated temperature of 60°C, density of low salinity water (can be any formulation) at different concentrations and crude oil must be identified. Table 6 summarizes properties of formation water at different temperatures, density of low salinity water at 1,000, 2,000, and 5,000 ppm and density of crude oil.

Table 6 Summary of fluid density and viscosity of formation water, at the concentration of 14,098 ppm, low salinity water formulations at 1,000, 2,000, 5,000 ppm and crude oil at 60°C

Fluid	Temperature (°C)	Density (g/cc)	Viscosity (cP)
Formation Brine	30	1.005	0.85
	60	1.004	0.40
Low Salinity Brine 1,000 ppm	60	1.000	0.40
Low Salinity Brine 2,000 ppm	60	1.001	0.40
Low Salinity Brine 5,000 ppm	60	1.002	0.40
Crude oil	60	0.79	4.18

4.2 Stirring Test

As many tests can be performed at the same time to the simplicity of the technique, it is preliminary used for screening water formulation. Grinded core sample was weighed for two grams and was stirred with 50 cm³ of low salinity water formulation. After stirring test, rock sample was removed from the mixture by using filter paper. Filtrate was taken for the titration process to identify: 1) total hardness of

solution; 2) concentration of calcium ion; and 3) concentration of ammonium ion remained in solution. Details of how ion concentrations being determined are described in section 4.2.1. However, the period of stirring must be identified and this is explained in section 4.2.2.

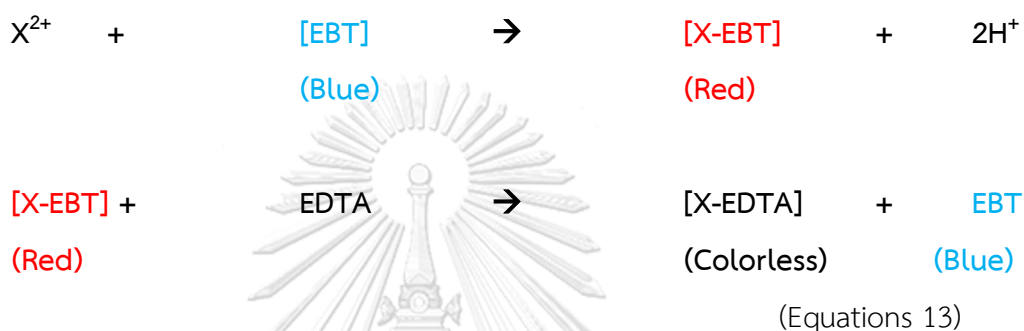
4.2.1 Determination of Ion Concentration by Titration

In order to confirm the most effective water formulation, it is expected to have the highest amount of divalent ions remaining in filtrate. Additionally, to support this first idea, ammonium which is believed to replace the site of divalent ion must be consumed during the process and high depletion amount of ammonium ion is expected. Determination of divalent ions can be separated to two processes which are the total hardness and concentration of only calcium ion.

To identify total hardness of filtrate, 10 cm³ of filtrate is pipetted into a conical flask, 3-4 drops of ammonium chloride/ammonia buffer solution was added together with a pinch of Eriochrome Black T (EBT) as an indicator. The mixture was vigorously swirled while titrating with 0.01M EDTA until the color of solution changes from red wine to sky blue. For concentration of calcium ion, 10 cm³ was pipetted into a conical flask. Sodium hydroxide solution with adequately high concentration was dropped into the flask to precipitate magnesium ions and pinch of hydroxynaphthol blue (HNB) was added into solution. Again, mixture was titrated with 0.01M EDTA until the color changes from red wine to blue sky. From these two color titrations, it is obligatory that total hardness is going to consume more amount of EDTA as total hardness is a combination of calcium and magnesium ion. Hence, concentration of magnesium ion can be obtained from the difference of these two titrations. Equations 13 and 14 express chemical reactions of how EBT and HNB change the color at end point.

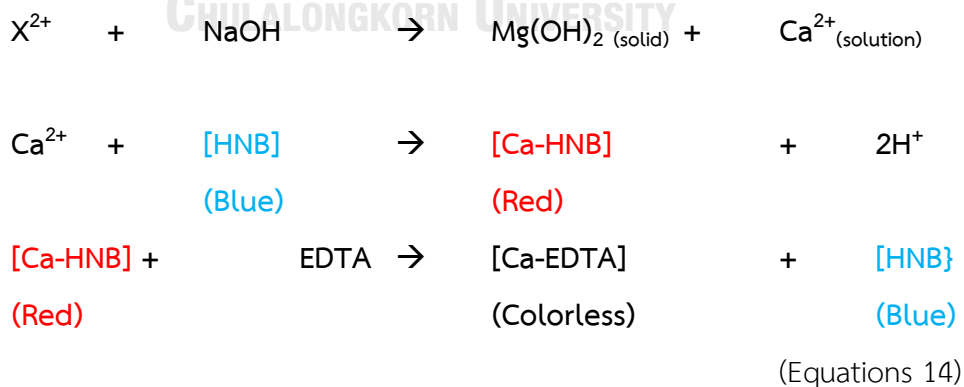
- Determining of the concentration of total hardness (Calcium ion and Magnesium ion or X^{2+})

The volume of EDTA used at the end-point represents the total concentration of Calcium ion and Magnesium ion existed in the filtrate. At the end of the titration test, the color changes from wine red to sky blue.



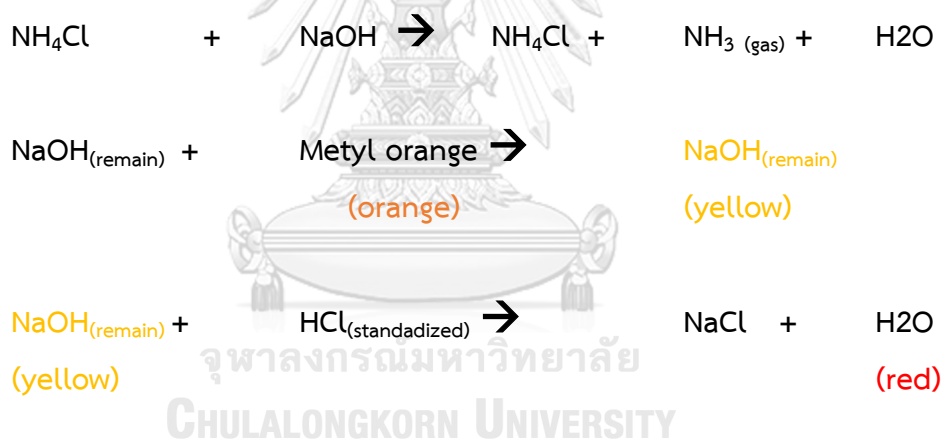
- Determining of the concentration of Calcium ion

The volume of EDTA used at the end-point shows the concentration of Calcium ion existed in the filtrate since Magnesium ion was precipitated by Sodium hydroxide. At the end of the titration test, the color changes from wine red to sky blue.



- Determining of the concentration of Ammonium ion

To identify the amount of ammonium ion, the back titration is performed. The technique starts with pipetting 10 cm³ of filtrate into a conical flask. A known concentration of sodium hydroxide is added and the mixture is heated for 2 hours to evaporate the ammonia gas which is a product from ammonium ion and sodium hydroxide. After that, the solution is titrated against standardized hydrochloric acid using methyl orange as an indicator. The end-point can be detected when color changes from bright yellow to red pink and the amount of ammonium remains is the different between initial concentration of sodium hydroxide and concentration after heating. Equations 15 expresses chemical reactions of how ammonium ion has been detected.



4.2.2. Determination of the Optimal Duration for Stirring Test

To ensure that the MIE mechanism during stirring test attains the equilibrium, the mixing duration is the key factor. The optimal time must be identified to ensure that obtained value will not be biased by stirring time and at the same time; total period should save the total experimental time. In this section solution of ammonium chloride at 1,000 ppm is used to stir with 2 grams of rock sample. Various stirring time is performed and filtrate is quickly tested for total hardness by complexometric titration with EDTA using EBT as an indicator (as explained in 4.2.1)

The stirring periods are 30 minutes, 1 hour, 2 hours, 4 hours, 6 hours and 8 hours. The optimal stirring time is selected from the time where the amount of total hardness starts to show the constant trend. Table 7 summarizes total hardness of filtrate solutions obtained from different stirring times.

Table 7 Summary of total hardness of filtrate solutions obtained from different stirring times

Test number	Stirring time (hr)	Volume of EDTA (cc)	Total hardness (ppm)
1	0.5	0.3	12
2	1	0.3	12
3	2	0.5	20
4	4	0.6	24
5	6	1.6	66
6	8	1.7	68

From Table 7 it can be observed that after 6 hours, total hardness strikingly increases from stirring time of 4 hours and the difference from stirring time of 6 hours to 8 hours is very small (2ppm). Therefore, stirring time of 6 hours is chosen as an optimal time for the entire study.

CHULALONGKORN UNIVERSITY

4.2.3 Determination of the Most Effective Water Formulation

As water formulation may be prepared from different sources of water and additional salt, combination of important ions therefore, becomes the most crucial parameter. In this study, ammonium is first selected to represent the interest ion followed by calcium ion which is found to be one of the potential determining ions during the MIE mechanism. Last, sodium ion which is the most abundant ion in formation water is also added into a system since the making of injected water may be based from diluting of formation water. Since, there are three important ions in this study; the result is represented by ternary diagram which is illustrated in Figure 5.

Each apex of the triangle represents a pure solution; for example, ammonium chloride solution, calcium chloride solution and sodium chloride solution for apex 1, 2 and 3 respectively. These three solutions are prepared to have the same salinity and any single point in this ternary diagram represents combination of these three solutions while keeping total salinity at the same as that of pure solution. In order to obtain results to cover all the area inside ternary diagram, 25 combinations of water formulations are prepared and Table 8 summarizes portions of each solution in order to make up water formulation.

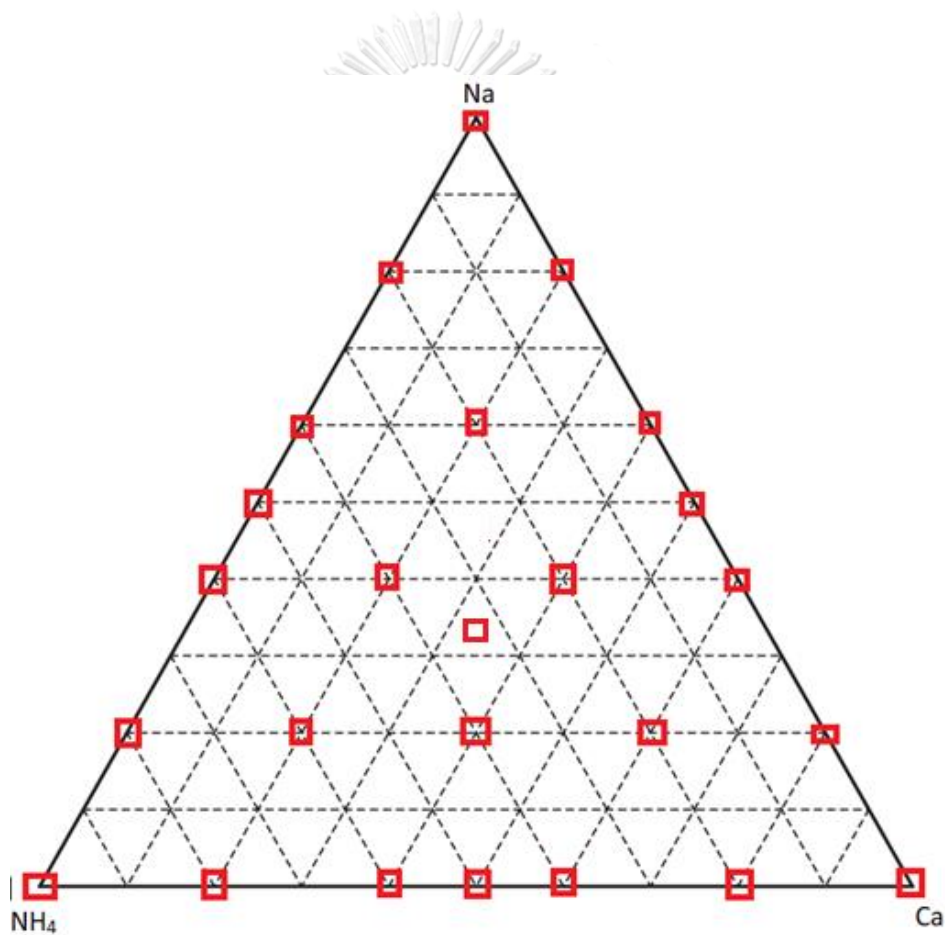


Figure 5 Example of ternary diagram illustrating three apex of ammonium chloride, calcium chloride and sodium chloride solutions and 25 combinations of water formulation to cover the whole area of diagram

Table 8 Volume portions of ammonium chloride, calcium chloride and ammonium chloride solutions to represent different 25 water formulations on ternary diagram

Case	Volume portion		
	NH ₄ Cl	CaCl ₂	NaCl
1	0	0	100
2	20	0	80
3	0	20	80
4	40	0	60
5	20	20	60
6	0	40	60
7	60	0	40
8	40	20	40
9	20	40	40
10	0	60	40
11	80	0	20
12	60	20	20
13	40	40	20
14	20	60	20
15	0	80	20
16	100	0	0
17	80	20	0
18	60	40	0
19	40	60	0
20	20	80	0
21	0	100	0
22	33.333	33.333	33.333
23	50	50	0
24	0	50	50
25	50	0	50

In one part of the study, potassium ion which is another monovalent ion that has similar capacity in MIE as ammonium ion will be added in the system and hence, a mixture of ammonium chloride and potassium chloride will be made at exact portion and this mixture will represent one apex of the new ternary diagram. The best water formulations are selected principally based on appearances of both calcium and magnesium ions. Moreover, disappearance of ammonium ion is additionally used to cross-check the MIE mechanism with the appearances of divalent ions.

4.3 Imbibition Test

Imbibition test is performed to assess the ability of certain ion to change wettability into a more water-wet condition through the MIE mechanism. Hence, the best water formulation will result into a fast imbibition rate. In this section, age core samples obtained from 4.1 are used. Core samples are soaked in different water formulations in different beakers. The beakers are then soaked in water bath system with controlled temperature at 60°C. This elevated temperature also helps preventing the wax precipitation of crude oil that could result in difficulty to the imbibition process.

As water imbibes into core sample, replacing oil out, weight of sample is increased due to the increment of water saturation. Weights of sample are then detected every 24 hours until the weight become constant, meaning that there is no more water imbibes into core sample. In order to change sample weight into fluid saturation, equations 4.6 to 4.7 are then utilized.

$$V_w = \frac{W_f - V_p \rho_o}{\rho_w - \rho_o} \quad (\text{Equation 15}),$$

$$S_w = \frac{V_w}{V_p} \quad (\text{Equation 16}),$$

where W_f is weight of fluid in core sample (gram), ρ_o is oil density (g/cm^3), ρ_w is water density (g/cm^3), and S_w is water saturation (fraction).

4.4 Coreflood Test

Coreflood test is performed to assess the effectiveness of low salinity water formulation in the most realistic conditions. The test is performed under high pressure and high temperature which are properties controlled by the coreflood apparatus. In this study, Flooding temperature is pre-set at 60°C and the confining pressure of 2,500 psi. The age core is placed into core holder and formation water is firstly injected at the rate of 0.5 cm³/min to imitate conventional waterflooding. After oil recovery factor remains constant for the period where 1.0 pore volume of liquid is injected, the process is switched to the injection of selected low salinity water until no more additional oil recovery is detected. Not only recoverable oil that is detected, effluent at the producing end is also collected for every 10 cm³ to identify appearances of calcium and magnesium ions and also disappearance of ammonium ion using techniques described in section 4.2.1. Figure 6 illustrates schematic diagram of coreflood apparatus including 5 important sections which are core holder section, confining pressure section, fluid injection section, back pressure regulator section and liquid separator section. In this study, the liquid separator section is not utilized as there are still several errors occur during the detection of liquid level. Hence, detection of liquid is performed by reading at the producing end.

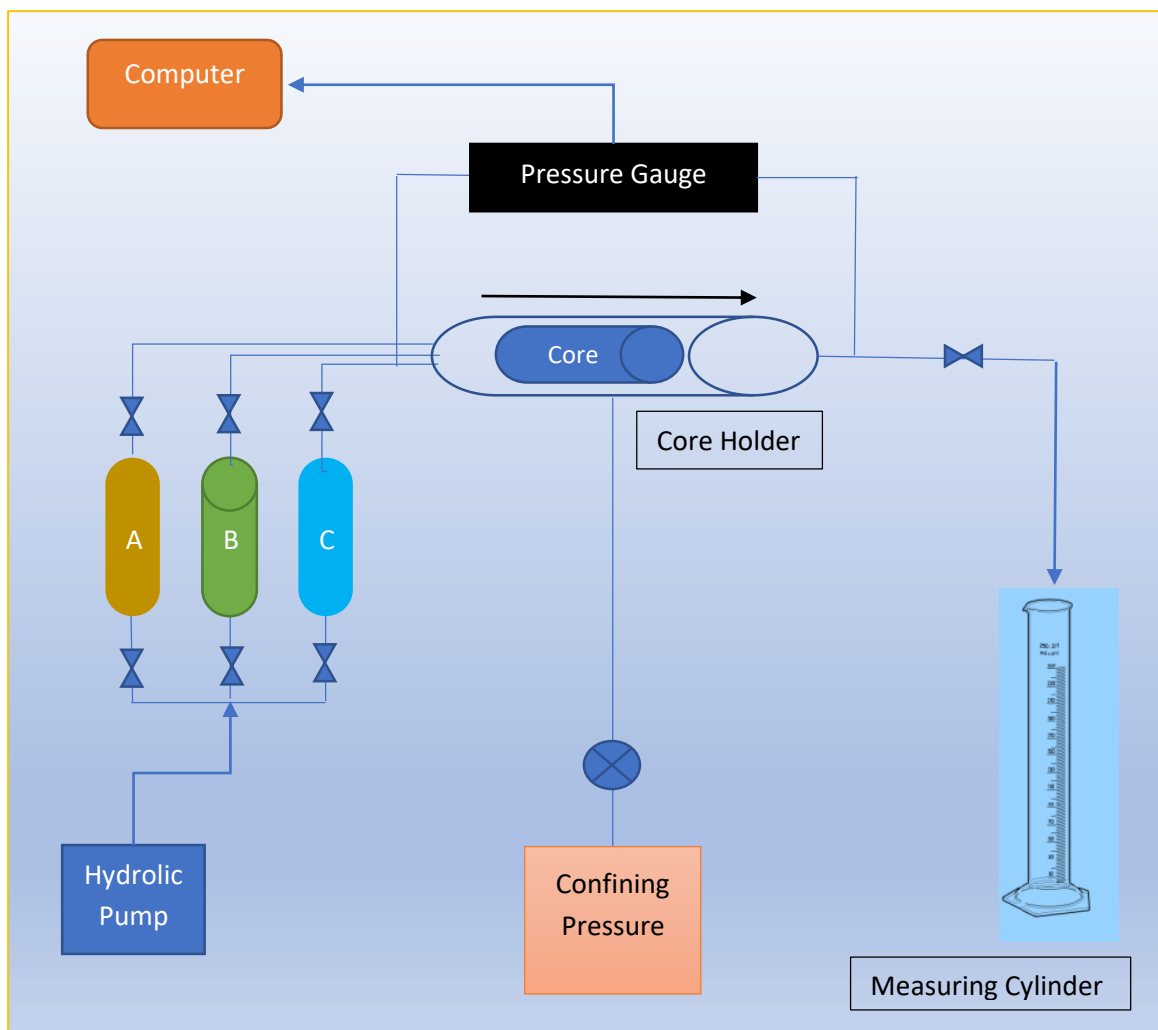


Figure 6 Schematic diagram of coreflood apparatus

4.5 Experimental Structure

This section summarizes the experimental structure together with the flow charts which are illustrated in Figures 7 to 9.

- 1) Perform stirring test of ammonium-calcium-sodium combinations at 1,000 ppm.
- 2) Repeat the task (1) at the total concentration of 2,000 and 5,000 ppm.

3) Select the best total concentration based on appearances of divalent ions together with disappearance of ammonium ion.

4) Perform stirring test of ammonium-potassium-calcium-sodium combination at the total concentration obtained in (3), using 2 different volume ratios of ammonium-potassium which are 4:1 and 1:4.

5) Select 4 water formulations and perform imbibition test and observe the increment of sample weights.

6) Perform coreflood tests with selected water formulations and detect oil recovery factors together with appearances of divalent ions and disappearance of ammonium ion in effluents.

7) Discuss the obtained results and conclude the new findings of the study.



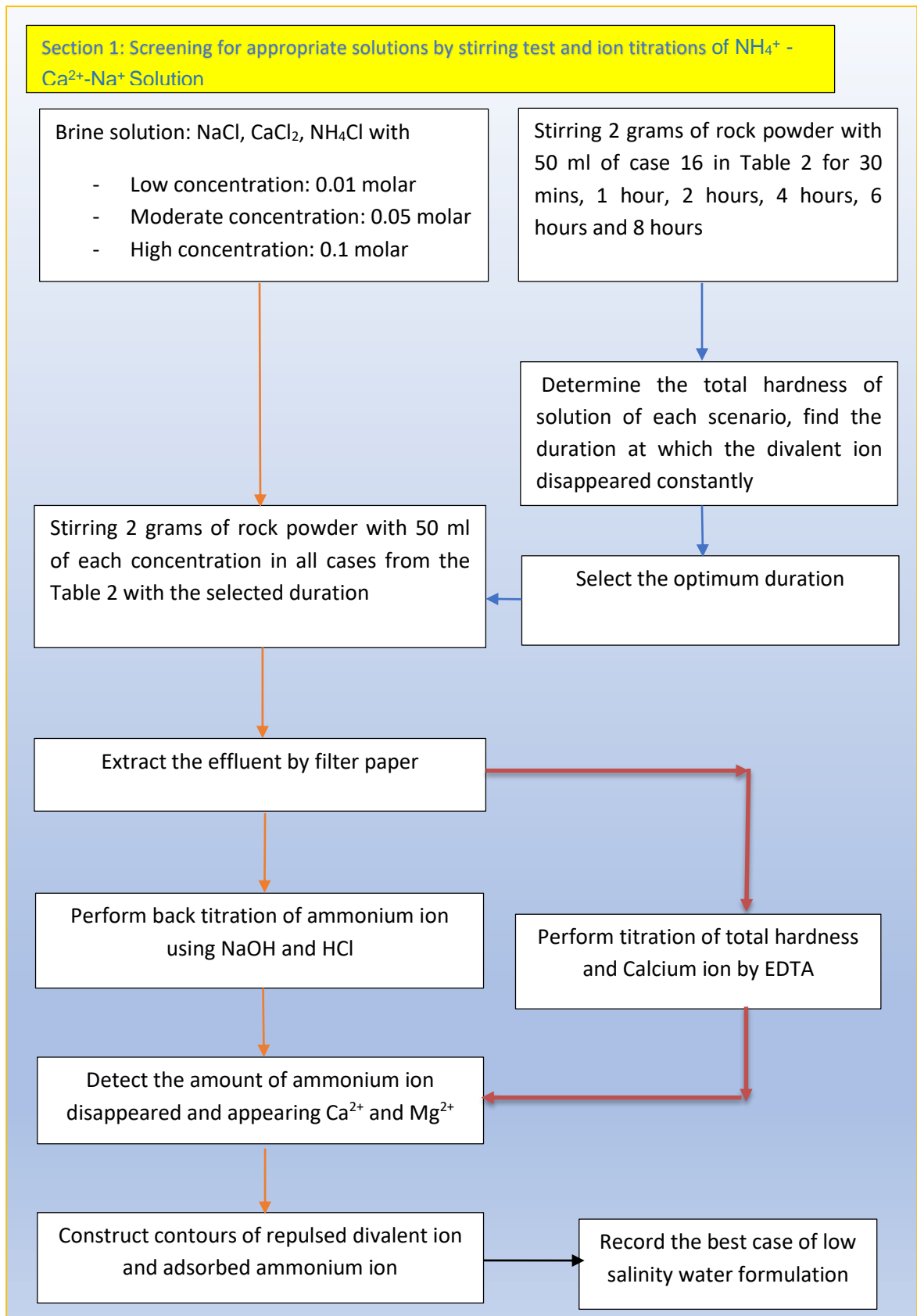


Figure 7 Summary of stirring test and ion titrations of NH_4^+ - Ca^{2+} - Na^+ solution

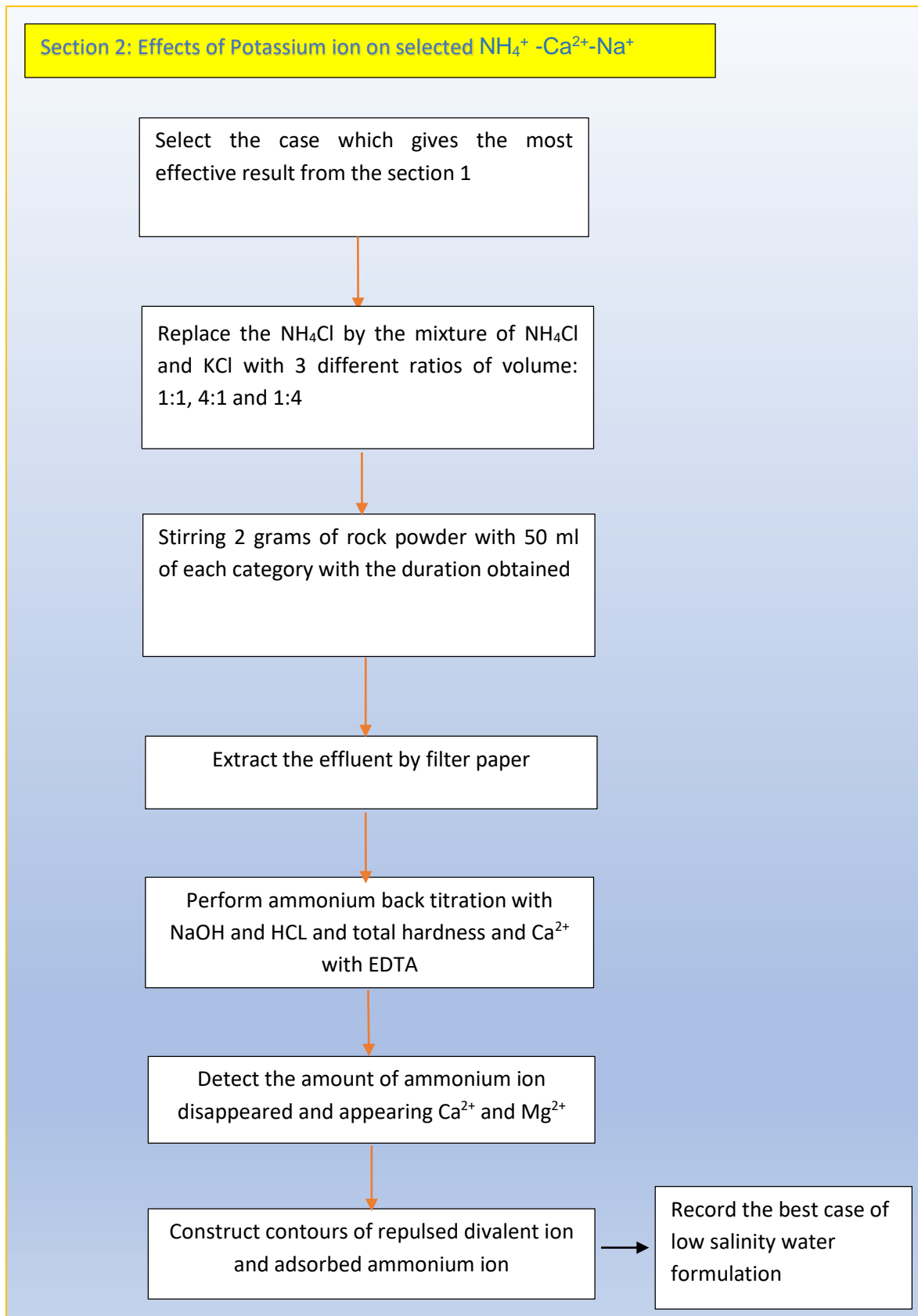


Figure 8 Summary of the effects of potassium ion in selected NH_4^+ - Ca^{2+} - Na^+ solution

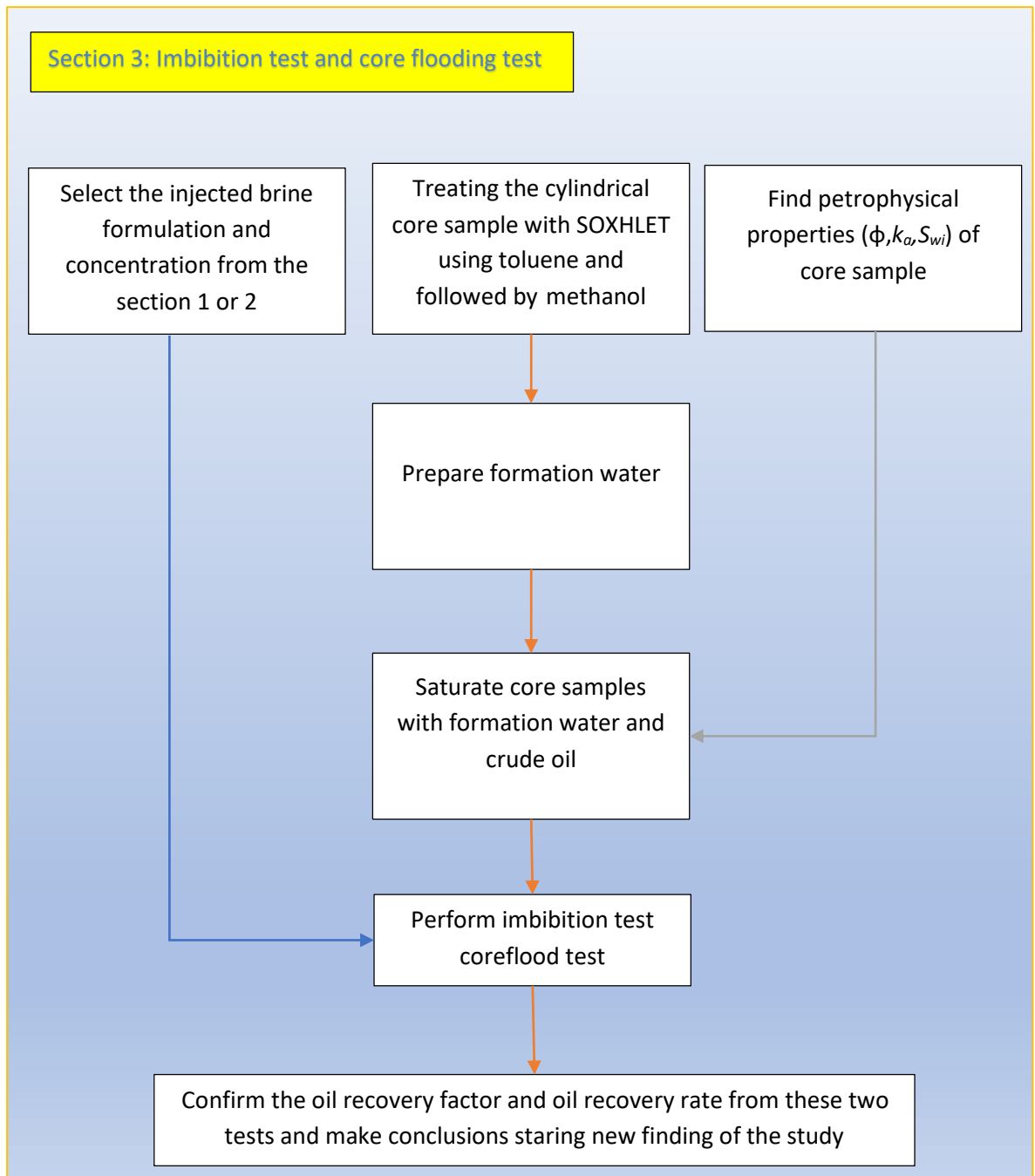


Figure 9 Summary of imbibition and coreflooding tests

CHAPTER V

RESULTS AND DISCUSSION

This section is separated into four sub-sections: 1) stirring test of ammonium-calcium-sodium combination and effects of total concentration; 2) stirring test of ammonium-potassium-calcium-sodium and effects of ammonium-potassium portion; 3) imbibition test and 4) coreflood test.

5.1 Stirring Test of NH_4^+ - Ca^{2+} - Na^+ Combination and Effects of Total Concentration

To observe the effect of MIE mechanism from injecting low salinity brine to the shaly-sandstone reservoir rock, the complexometric titration test and back titration test are performed. The volume of EDTA as the titrant of complexometric and the volume of sodium hydroxide as the titrant of back titration are recorded. They are the input data to Python Scripts to create ternary diagrams, which are the chart in triangular shape, to represent the percent of each components in water formulation and the concentration of the target titration at the same time.

5.1.1 Explanation of NH_4^+ - Ca^{2+} - Na^+ Ternary Diagram

From the stirring tests, the results of total hardness, calcium concentration titration and ammonium ion back titration are collected and the ternary diagrams are constructed for dissolution of calcium ion, dissolution of magnesium ion and adsorption of ammonium ion. Total hardness is a summation of calcium and magnesium ions whereas the difference of EDTA volume from total hardness test and calcium concentration titration test results in the amount of magnesium ion. Figure 10a illustrates appearance of calcium ion and figure 10b depicts appearance of magnesium ion, while the concentration of ammonium ion consumed obtained from back titration is in the Figure 10c.

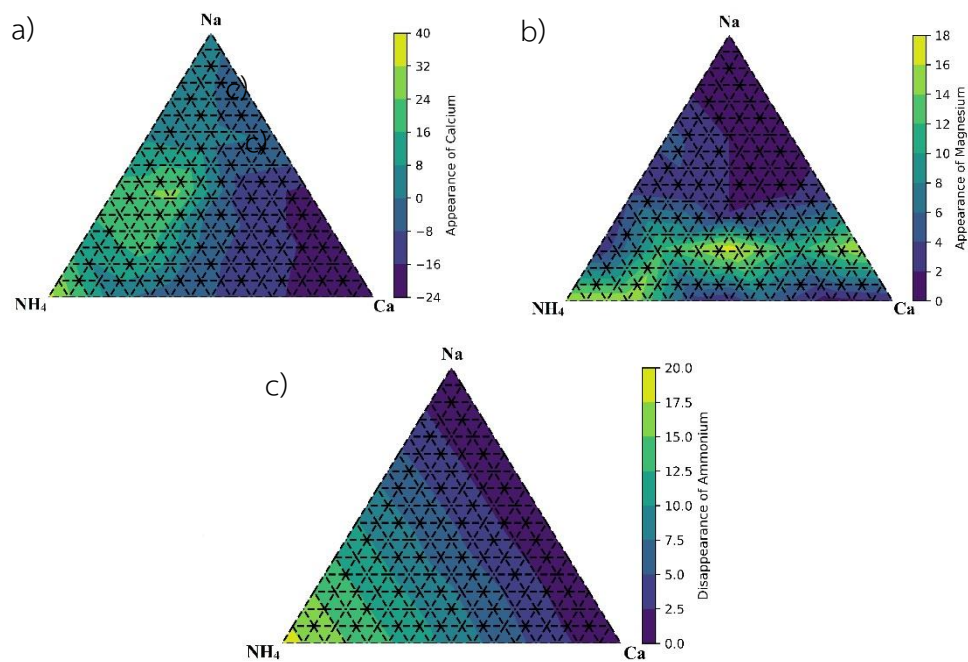


Figure 10 Ternary phase diagrams illustrating appearance of a) calcium ion and b) magnesium ion ; c) disappearance of ammonium ion of formulation brine containing ammonium-calcium-sodium at 1,000 ppm

As can be seen from figure 10a, the water formulations which contains less amount of calcium ion tends to yield the highest amount of calcium ion which could be explained by dissolution mechanism. Especially the combination between sodium ion and ammonium ion shows positive result when the concentration of calcium ion is low. Moreover, the positive magnitude appears at the pure ammonium ion. The explanation is included by two different methods. First, these two monovalent ions can fulfill the MIE mechanism during low salinity injection as they can displace the divalent ions such as calcium ion. Second, potassium ion which is enriched in clays may be dissolved in aqueous solution especially when concentration of sodium ion is higher and this potassium ion can undergo the MIE process as potassium ion has similar characteristics as ammonium ion. On the other hands, when the calcium ion increased, calcium ion disappears. Considering figure 10b, appearance of magnesium

ion can be related to the disappearance of calcium ion. Appearance of magnesium ion can be explained by two major mechanisms. When concentration of ammonium is high, ammonium ion does not replace only calcium ion, but it can also replace magnesium ion. When amount of calcium ion is increased, calcium ion can assist replacing of magnesium ion at the same time. Nevertheless, it is obvious that appearance of magnesium ion is independent from concentration of sodium ion. Last, disappearance of ammonium ion shown in figure 10c illustrates that higher concentration of ammonium ion results in higher adsorption of ammonium ion itself. As ammonium ion is a foreign ion or it does not exist in clay mineral as other monovalent ion such as potassium ion or sodium ion, its adsorption is therefore dependent only with its concentration is surrounding water.

5.1.2 Effects of Total Concentration on NH_4^+ - Ca^{2+} - Na^+ Ternary Diagram

To detect the effect from salt concentration on MIE mechanisms, water formulations are additionally prepared to have total hardness of 2,000 ppm and 5,000 ppm. Starting with total hardness of 2,000 ppm, figures 11 a, b and c, illustrate ternary diagrams of appearance of calcium ion, appearance of magnesium ion and disappearance of ammonium ion, respectively. Comparing with total concentration of 1,000 ppm, appearance of calcium ion is more obvious at the total concentration of 2,000 ppm; the higher the calcium ion concentration, the higher the disappearance of itself. The disappearance of magnesium ion also shows a similar tendency as total concentration of 1,000 ppm. The only difference is the appearance of magnesium ion. Great amount of magnesium ion is not observed in two conditions: 1) mixture of calcium ion and ammonium ion without sodium ion and 2) mixture of calcium ion and sodium ion (with higher portion of calcium ion than sodium ion). For case 1) as there are both ammonium and calcium ions at adequate concentration, the MIE can occur to release magnesium ion. The shifting of the high magnesium ion zone in figure 10b to the bottom of ternary diagram in figure 11b can be explained that at higher concentration, there are enough monovalent ion which is ammonium ion and it does not need potassium ion dissolution which may relate to the presence of

sodium ion. For case 2), the presence of sodium calcium ions may result in dissolution of potassium ion and that could complete the MIE without participation of ammonium ion.

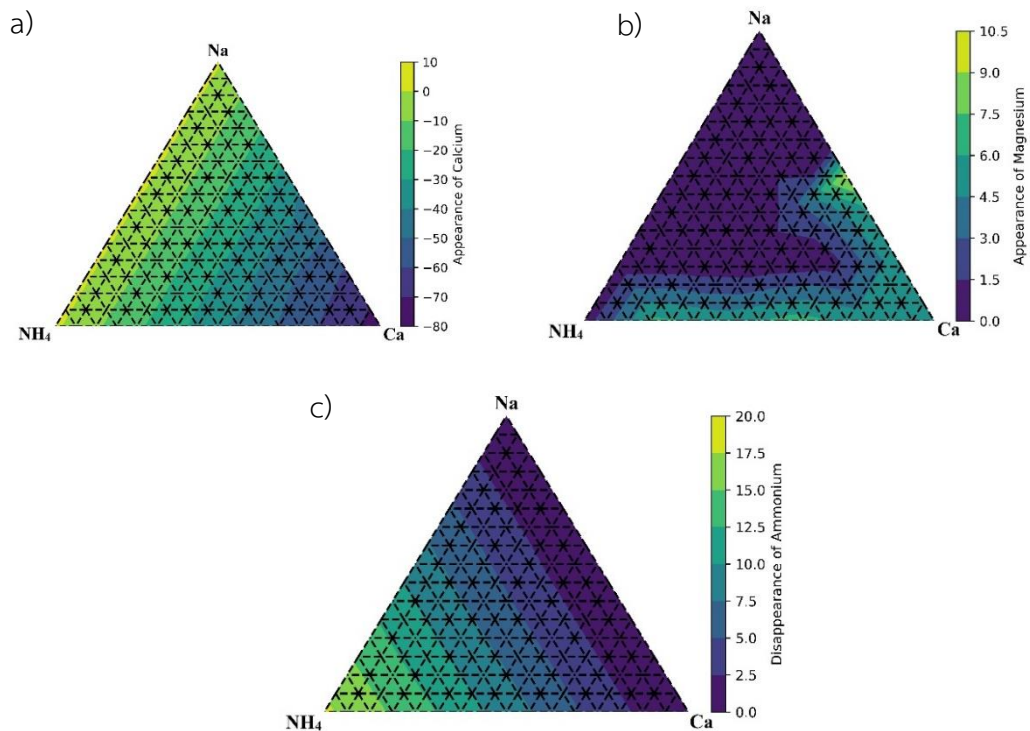


Figure 11 Ternary phase diagrams illustrating appearance of a) calcium ion and b) magnesium ion; c) disappearance of ammonium ion of formulation brine containing ammonium-calcium-sodium at 2,000 ppm

At the higher concentration of 5,000 ppm, characteristics of appearance of calcium and magnesium ions and disappearance of ammonium ion are similar to those obtained from the cases of total concentration of 2,000 ppm. Figures 12 a, b, and c illustrate appearance of calcium ion, appearance of magnesium ion and disappearance of ammonium ion, respectively. A slight difference can be observed in the appearance of magnesium ion at low calcium ion concentration and approximately half-half of ammonium and sodium ion concentration. Since this location only appears in one spot in the graph, it could be possible that the rock sample used for stirring test may contain the abnormally high clay percent that may

cause high release of potassium ion that consecutively results in replacing of magnesium ion.

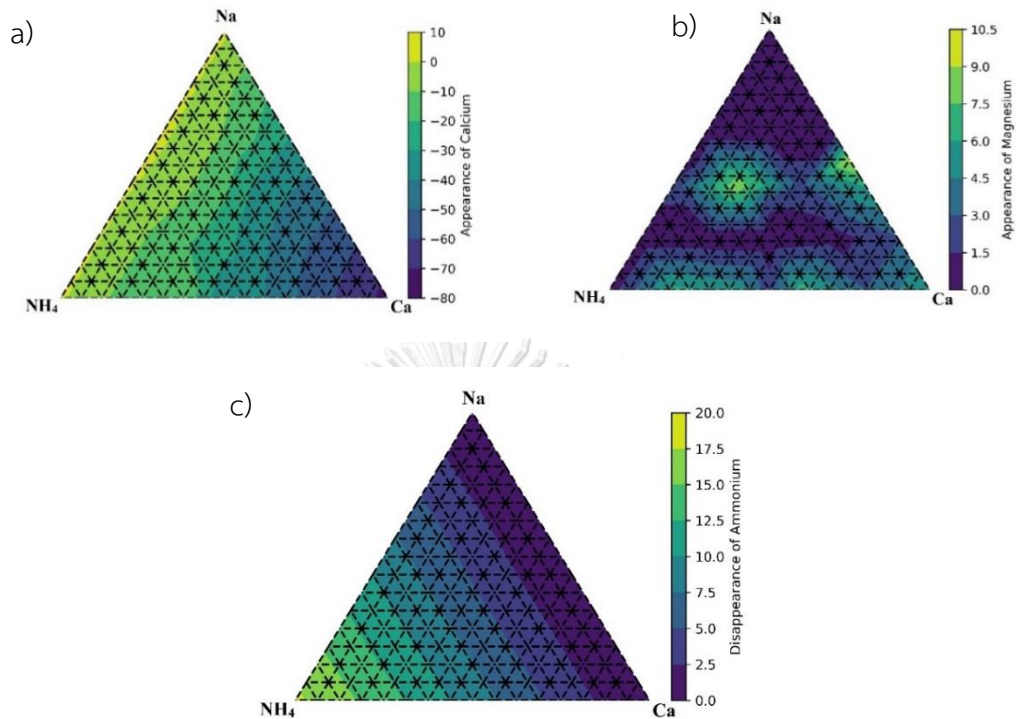


Figure 12 Ternary phase diagrams illustrating appearance of a) calcium ion and b) magnesium ion; c) disappearance of ammonium ion of formulation brine containing ammonium-calcium-sodium at 5,000 ppm

From the stirring test and titrations in this section, it is obvious that the total concentration of 1,000 results in high dissolution of calcium and magnesium ions. Therefore, the concentration of 1,000 ppm is chosen for the following sections in this study.

From the appearance of divalent ions and disappearance of ammonium ion, it results in a summary of ionic activities at 1,000 ppm in figure 13. From the figure, different concentrations of different ions result in several explanations. In zone A, majority of sodium ion replaces calcium ion, but sodium ion cannot replace any magnesium ion. Zone B witnesses the combination of ammonium and sodium ions

and due to lacking calcium ion, dissolution of calcium ion is remarkable in this region. It is noted that in this zone B, potassium ion may release to assist the replacing of calcium ion. However, according to the data in zone C, appearance of magnesium ion is the highest as a result from replacing of both ammonium and calcium ions. Zone D which is the zone enriching of calcium ion concentration, results in dissolution of magnesium ion that is from replacement by calcium ion together with potassium ion from the clay itself. In the system lacking sodium ion, zone E represent the worst activity. This can be explained that at very low salt concentration, ammonium and calcium ion may not be enough to trigger the MIE mechanism and especially without sodium ion dissolution of sodium ion from clay instead of dissolution of other important ions for MIE. Last, high concentration of ammonium ion and absent of calcium ion in zone F seems to be one of the desirable zones. The highest disappearance of ammonium ion results in dissolution of both calcium and magnesium ions. Moreover, when total concentration increases, it seems that Figure 10 may slightly change especially for zone C that may move downward to replace zone E and merge with zone D.

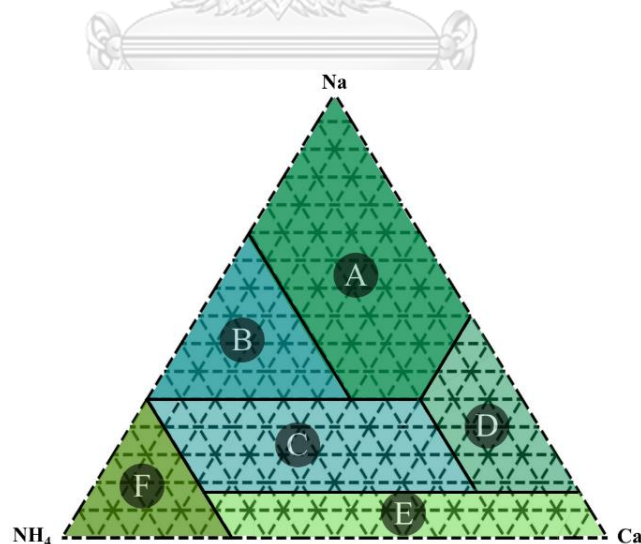


Figure 13 Ternary phase diagrams illustrating zones of ion activities on shaly-sandstone sample based on concentration of ammonium ion, sodium ion and calcium ion at the concentration of 1,000 ppm

5.2 Stirring Test of Ammonium-Potassium-Calcium-Sodium Combination and Effects of Ammonium-Potassium Portion

Based on several previous researches in low salinity waterflooding using monovalent ions, potassium ion has been proven as a potential ion to add into low salinity water. The idea has been generated to mix ammonium ion and potassium ion in certain portions, in order to inspect if these two monovalent ions can work in collaboration while injecting low salinity water into shaly-sandstone reservoir. The concentration of 1,000 ppm is applied through these experiments since it showed the most positive results in complexometric test among other concentrations. The test is performed by mixing 2 grams rock powder with low salinity water containing ammonium chloride/potassium chloride (in certain ratios), calcium chloride and sodium chloride. Two ratios between ammonium ion and potassium ion chosen in this study are ammonium-potassium = 4:1 and ammonium-potassium = 1:4.

5.2.1 Low Ammonium Ion Portion (Ammonium-Potassium of 1:4)

Figures 14 a, b, and c depict the appearances of calcium ion, magnesium ion and the disappearance of ammonium ion. Comparing figure 14a and figure 10a it can be observed that when ammonium ion is replaced by potassium ion, appearance of calcium ion is mostly disappeared from the diagram. Nevertheless, from figure 14b, it can be observed that the area where magnesium ion is produced increases. This is an evidence that ammonium ion tends to displace calcium ion whereas potassium ion tends to displace magnesium ion when calcium ion is also found in the system. The highest value of magnesium ion concentration is observed at $\text{NH}_4\text{-Ca-Na}$ is 20-80-0; however, It is obviously seen from the figure 14b that the differential dissolution range of magnesium ion (12-14) is still smaller than the formulation without potassium ion (16-18) in the figure 10b

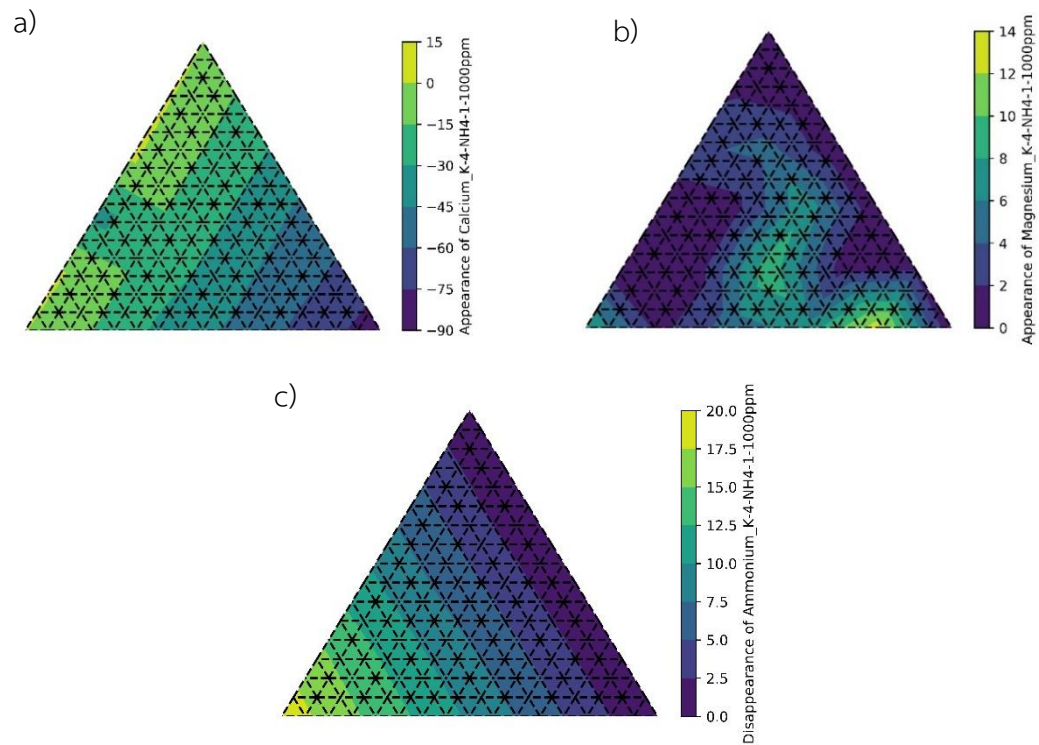


Figure 14 Ternary phase diagrams illustrating appearance of a) calcium ion and b) magnesium ion; c) disappearance of ammonium ion of formulation brine containing ammonium/potassium chloride – calcium chloride – sodium chloride at 1,000 ppm

Due to the effect from potassium ion which already existed in the shaly-sandstone formation and majority of monovalent ion which is potassium ion, the influence of ammonium ion is less. As a result, most of the released magnesium ion is from collaboration of potassium and calcium ions.

5.2.2 High Ammonium Ion Portion (Ammonium-Potassium of 4:1)

Figures 15 a, b, and c illustrate appearance of calcium and magnesium ions and disappearance of ammonium ion. From figure 15a it can be seen that the dissolution of calcium ion is nearly the same as in the case with low ammonium ion. However, the area around pure ammonium-potassium solution results in larger

positive value of calcium ion in the solution. In aspect of magnesium ion appearance as shown in figure 15b, the profile shows similar trend as in previous case. However, the magnitude of maximum appearance is reduced to just 9-10.5 ppm at the combination of $\text{NH}_4\text{-Ca-Na}$ is 40-40-20. As explained previously in 5.2.1, presence of potassium ion tends to shift the displacement from calcium to magnesium ion. However, potassium ion may also replace calcium ion as ammonium ion but it may collaborate with calcium ion to replace consecutively magnesium ion.

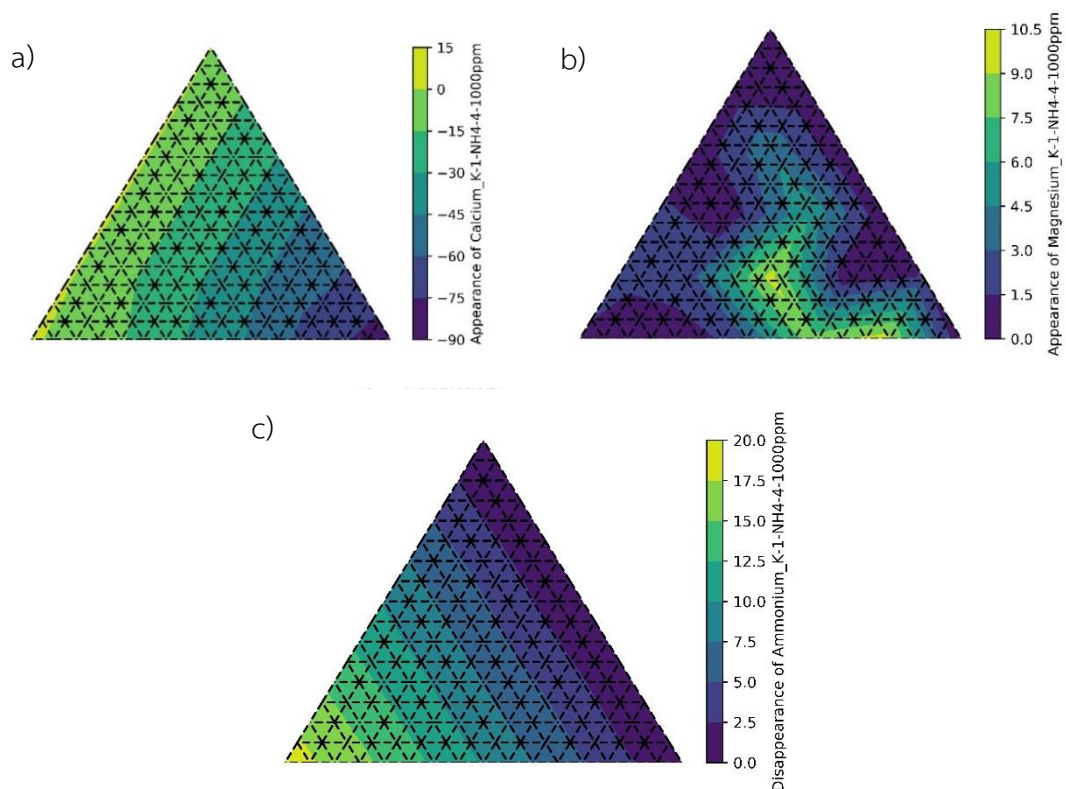


Figure 15 Ternary phase diagrams illustrating appearance of a) calcium ion and b) magnesium ion; c) disappearance of ammonium ion of formulation brine containing ammonium/potassium chloride – calcium chloride – sodium chloride at 1,000 ppm

In conclusion, it can be observed that replacing ammonium ion by potassium ion tends to shift the replacement from calcium ion to magnesium ion. However, the magnitude of magnesium ion in case that potassium ion is added is still less than the

case of pure ammonium. This can be explained that, ammonium ion can replace very well calcium ion and consecutively, this abundant of calcium ion would continue to replace high amount of magnesium ion. Therefore, the mixing of potassium ion would result in reducing ability of ammonium ion even though ammonium ion may not replace directly well the magnesium ion.

For the following session including imbibition and coreflood tests, these cases are selected: 1) formation water; 2) pure ammonium chloride at 1,000 ppm; (3) water formulation at 1,000 ppm containing ammonium chloride 40%, calcium chloride 40% and sodium chloride 20%; and (4) water formulation at 1,000 ppm containing ammonium chloride 40%, calcium chloride 20% and sodium chloride 40%.

Case 1 is selected as blank test for imbibition case and to perform in all coreflood tests prior to the selected water formulation. For the case 2), the purpose is to identify the effect of ammonium in MIE mechanism without an assist of calcium ion and sodium ion. In case 3), the expected result is to observe when high portion of calcium ion is found in solution whereas case 4), it aims to assess displacement mechanism when magnesium ion is well released.

5.3 Imbibition Test

The imbibition test is performed to investigate the wettability alteration which is related to Multi-component Ions Exchange (MIE) mechanism. In shaly-sandstones reservoir, the initial wettability condition is expected to be oil-wet as divalent ions in clay may form interaction with acid in crude oil. Therefore, spontaneous imbibition cannot be happened easily. When rock surface is in contact to different water formulations, MIE may take place which means wettability should shift toward new equilibrium.

If formation water is applied for imbibition test, the same salinity and as well as ion composition would result in difficulty for wettability to shift to a new equilibrium and the spontaneous imbibition will occur slowly. On the contrary, if the total salinity and chemical composition of water are modified to favor oil recovery mechanism, this low salinity water will shift quickly the wettability to water-wet

condition and hence, spontaneous imbibition will start quickly into rock sample. In this study, there are 4 water formulations which are chosen from the previous sections which are: 1) synthetic formation water at 14,098 ppm; 2) low salinity water containing ammonium chloride at 1,000 ppm; 3) low salinity water at 1,000 ppm with ratio of ammonium-calcium-sodium is 40-40-20; and 4) low salinity water at 1,000 ppm with ratio of ammonium-calcium-sodium is 40-20-40. Table 9 summarizes composition of formation water matching with specific core number whereas Table 10 summarizes composition of 3 different low salinity water formulations.

Table 9 Ions compositions of formation water

Ions	Core	Mol/L	g/L	ppm
Na ⁺	44	0.22055	5.07265	5072.6
Ca ²⁺		0.00636	0.2544	254.4
Mg ²⁺		0.00116	0.02784	27.8
K ⁺		0.00215	0.08385	83.8
HCO ₃ ⁻		0.00856	0.52216	522.1
Cl ⁻		0.22919	8.1362	8136.2
Total ppm				14,098

Table 10 Ions composition of three different selected low salinity water formulations

Ratios of ammonium - calcium - sodium	Core	Ions	Mo/L	g/l	ppm
100:0:0	19	NH ₄ ⁺	0.01869	0.3365	336.5
		Cl ⁻	0.01869	0.6635	663.5
Total salinity					1,000
40:40:20	17	NH ₄ ⁺	0.00747	0.13446	134.46
		Ca ²⁺	0.0036	0.1441	144.1
		Na ⁺	0.00341	0.0786	78.6
		Cl ⁻	0.01808	0.6418	641.8
Total salinity					1,000
40:20:40	25	NH ₄ ⁺	0.00747	0.13446	134.46
		Ca ²⁺	0.0018	0.072	72
		Na ⁺	0.006837	0.1572	157.2
		Cl ⁻	0.0179	0.6357	635.7
Total salinity					1,000

The results from spontaneous imbibition tests is obtained by soaking each core sample into its correspondent water formulation. Each core sample is weighed at the same period every day until weight of the samples are constant. Together with core data and recorded weights, water saturations can be identified from calculation (equation 4.6 and equation 4.7) and recovery factor for each case is summarized in Table 11.

Table 11 Summary of recovery factors obtained from imbibition tests of different core samples in different water formulations at different time

Sample	Brine	Day 0	Day 1	Day 2	Day 3	Day 4	Day 5	Day 6
44	Formation water	0.000	0.000	0.027	0.038	0.038	0.038	0.038
19	Ammonium Chloride 1,000 ppm	0.000	0.000	0.186	0.233	0.233	0.233	0.233
17	NH ₄ /Ca/Na = 40/40/20	0.000	0.000	0.022	0.059	0.124	0.124	0.124
25	NH ₄ /Ca/Na = 40/20/40	0.000	0.007	0.007	0.014	0.040	0.081	0.081

As can be seen from the table, oil recovery factor gained is quite small when performing imbibition test using formation water. Meanwhile, for other low salinity waters, recovery factors at each day is obviously higher. At the end of the test, formation water can recover only 3.8%, while 8-23% of oil recovery can be obtained from low salinity water formations at 1,000 ppm. It can be obviously noticed that water formulation containing only ammonium chloride at 1,000 ppm showed the highest recovery of 23.3% oil recovery factor. As ammonium ion is monovalent ion that does not exist in rock surface, so it can be easily adsorbed onto mineral surface, causing the propagation of MIE mechanism as well as spontaneous. For the cases, oil recovery factor is 12.4% and 8.1% for cases of NH₄/Ca/Na = 40/40/20 and NH₄/Ca/Na = 40/20/40, respectively.

Besides, the differential water saturation of each core and brine is also calculated and the plot versus time shows the velocity of water formulations that can imbibe into the core samples. Figure 16 represents the result from imbibition test in the relationship between differential saturation versus soaking time.

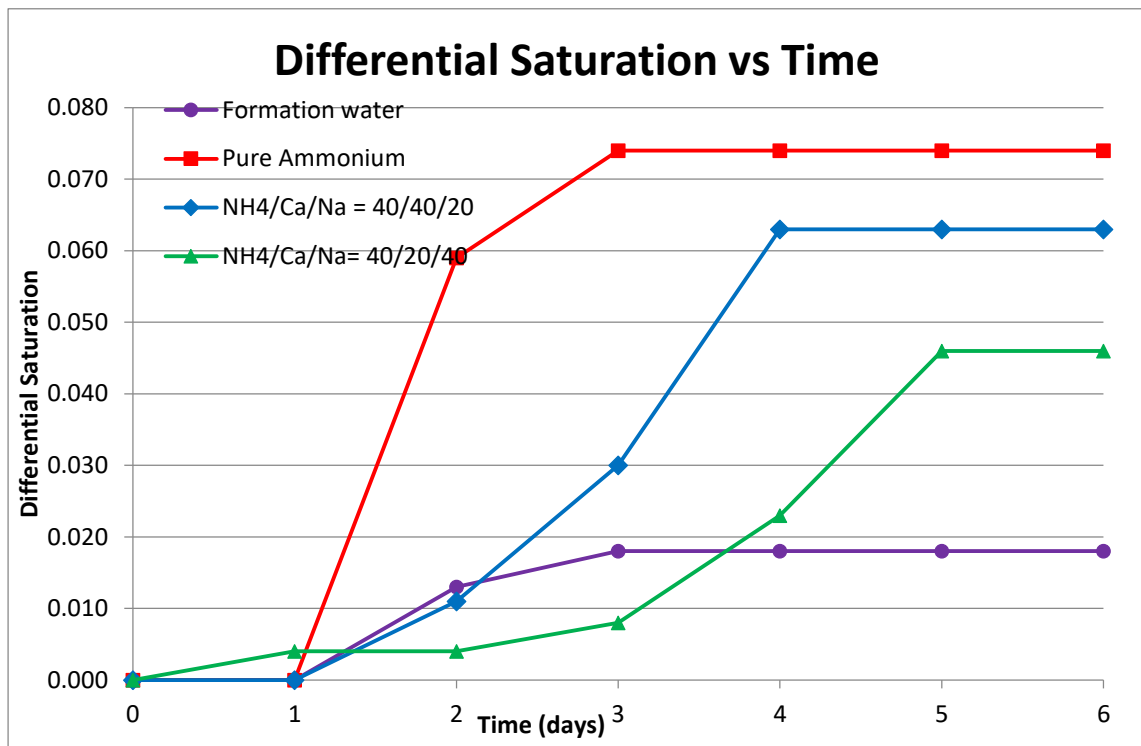


Figure 16 Differential water saturation versus soaking time of four core samples tested with different water formulations

From the results in this section, it can be obviously seen that low salinity water can cause much better spontaneous imbibition compared to formation water. Nevertheless, the magnitude of oil recovery is very small since the test of imbibition test tends to neglect viscous force from the injection rate. Hence, only capillary force and gravity forces are taken place. All three selected water formulations express an ability to imbibe spontaneous that means they can cause the MIE mechanism and change wettability of rock samples. However, it is still difficult to judge in this stage that which solution is better than others since core samples are not the same and hence, the imbibition rate may be influenced by other properties that are difficult to control such as permeability, pore structures, heterogeneity of rock sample and percentage of clays in core samples. Nevertheless, it can be concluded that the selected three water formulations would positively result in the next step.

5.4 Coreflood Test

5.4.1 Recovery Factors

In coreflood tests, viscous force is also included and the testing conditions are similar to that occurs in reservoir conditions. In this section, core sample is flooded by formation water until oil is no longer produced. After that, the process is switched to low salinity water flooding. Hence, only three core samples are selected for this section. Table 12 summarized important properties of 3 core samples for three chosen water formulations and table 13 summarizes composition of water formulations for different cases.

As previously describe in chapter 4, coreflood experiments are performed at certain conditions: temperature are set at 60 degree Celsius with confining pressure of 1,500 psi. Injection rate is maintained constant at 0.5 cm³/min in both conventional flooding and low salinity waterflooding.

Table 12 Characteristics of core sample used in coreflooding test

Core	Pore Volume (cm ³)	S_{oi}	Permeability
44	17.18	17.87	181.01
17	15.21	15.21	52.91
25	13.28	13.28	25.11

Table 13 Ions component of low salinity brines in the coreflooding test

Ratios of NH_4^+ and Ca^{2+} and Na^+	Core	Ions	Mo/L	g/l	ppm
100:0:0	25	NH_4^+	0.01869	0.3365	336.5
		Cl^-	0.01869	0.6635	663.5
40:40:20	17	NH_4^+	0.00747	0.13446	134.46
		Ca^{2+}	0.0036	0.1441	144.1
		Na^+	0.00341	0.0786	78.6
		Cl^-	0.01808	0.6418	641.8
40:20:40	44	NH_4^+	0.00747	0.13446	134.46
		Ca^{2+}	0.0018	0.072	72
		Na^+	0.006837	0.1572	157.2
		Cl^-	0.0179	0.6357	635.7

In this section, three cores are selected which are core 25, core 17 and core 44 due to their good characteristics which are pore volume, permeability and initial oil saturation. Core 19 is not selected due to too small amount of initial oil saturation (too high irreducible water saturation) which could lead to the difficult to assess the effectiveness of low salinity water formulation.

Figure 17 illustrates oil recovery factor together with pressure difference across core sample during the experiment using pure ammonium solution as injected low salinity water.

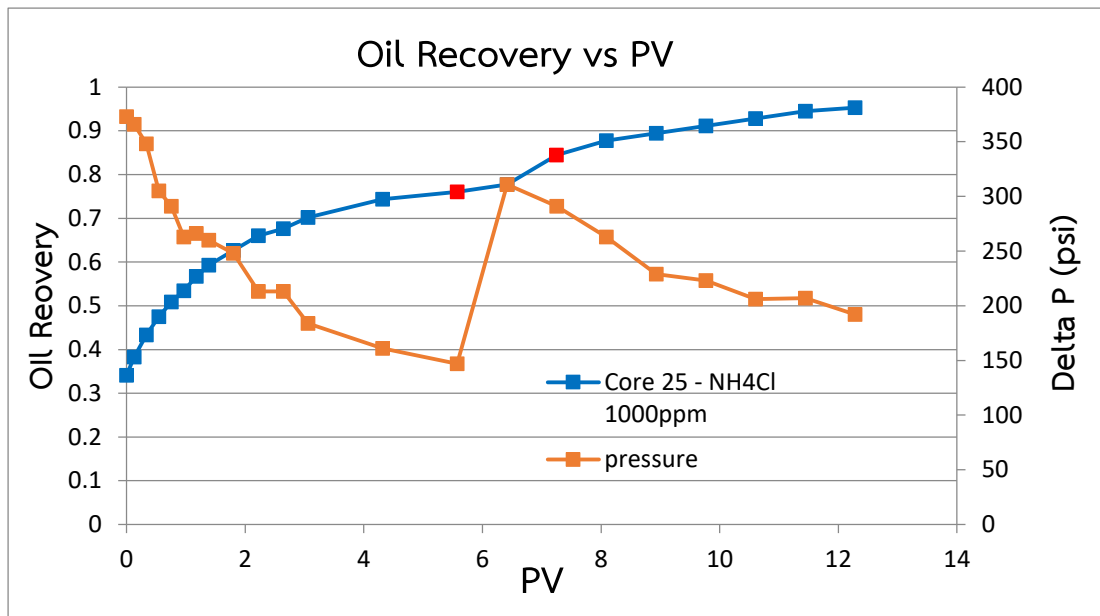


Figure 17 Oil recovery factors from coreflood tests obtained from low salinity water containing ammonium chloride at 1,000 ppm

From figure 17, oil recovery increases strikingly in first period (0-2 pore volume of conventional waterflooding). After that, oil is less produced and water production increased. At the end of conventional waterflooding, recovery factor is approximately to 0.76, Low salinity water is injected before the 6.4 injected pore volume which is represented by first red point on the left-hand side of the switching LSWF point. After less than 2 PV of low salinity water (pure ammonium chloride solution), new oil bank starts and this results in an obvious increment of oil recovery factor (second red point on right hand side of the switching LSWF point). After low salinity waterflooding oil recovery goes up to 0.95 which is approximately 19% incremental after conventional waterflooding. From the data of pressure difference, it can be observed that pressure different increases by two times when formation water is switched to low salinity water. This can be explained that suddenly after injection of low salinity water, MIE may occur and oil is liberated together with new rearrangement of ions. As a result, liberated oil causes the difficulty for the flow path and eventually results in increment of pressure difference. One more interesting thing can be seen is that, after formation water is switched to low salinity water, the effect of salinity water will

appear by the color of effluent. Water will change from colorless to a turbid pale yellow that could be explained by the MIE mechanism, resulting in stabilization of small oil drop in aqueous phase.

Figure 18 illustrates results including oil recovery factor and different pressure obtained from the solution $\text{NH}_4\text{-Ca-Na}$ of 40-40-20 which is the formulation expected to release higher portion of magnesium ion.

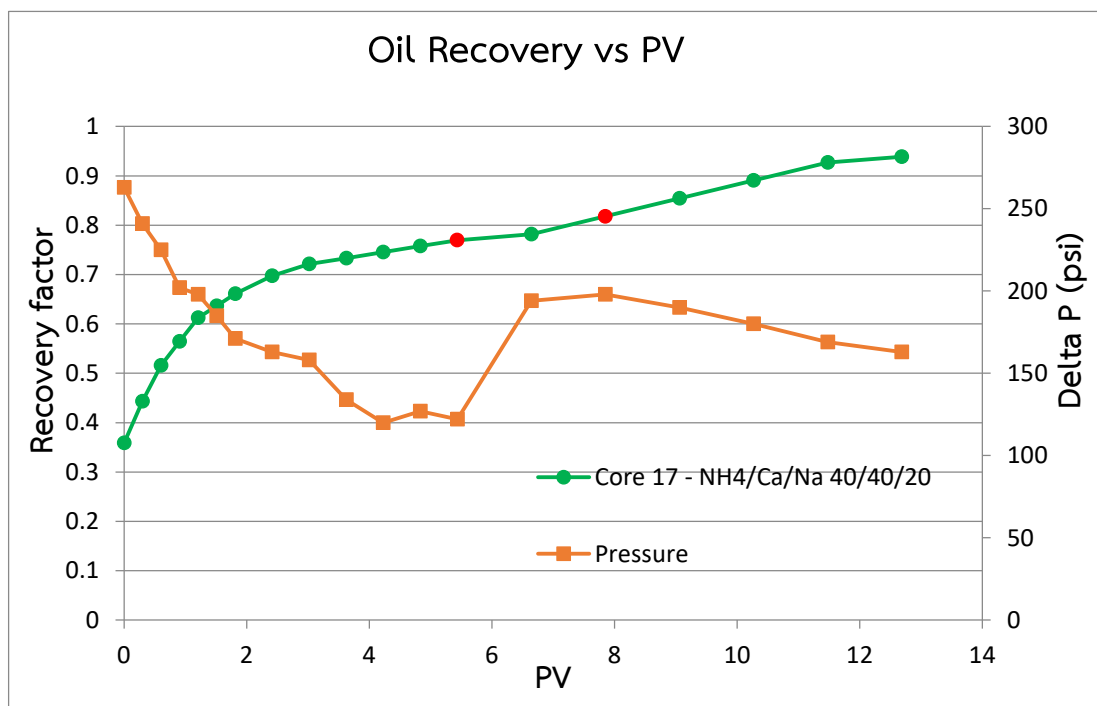


Figure 18 Oil recovery factors from coreflood tests obtained from low salinity water containing ammonium chloride- calcium chloride – sodium chloride at ratio of 40-40-20

As can be seen in Figure 18, the increment of oil due to low salinity water is still observed but it is not as high as the previous cases. The period from starting time to the first time to observe effect from low salinity water takes more than 2PV of injected fluid. Moreover, at the time where formation water is switched to low salinity water, pressure difference does not increase strikingly as in previous case. By conventional waterflooding, recovery factor is 0.77 at the end of low salinity

waterflooding, oil recovery is increased to 0.94 which accounts for 17% incremental. As this water formulation tends to release magnesium ion more than calcium ion, this can be explained that most oil that is linked through magnesium ion may be difficult to undergo the MIE mechanism since the ionic radius of magnesium is very small. The selected solution therefore can improve oil recovery with less potential compared to the pure ammonium solution.

Figure 19 depicts results including oil recovery factor and different pressure obtained from the solution $\text{NH}_4\text{-Ca-Na}$ of 40-20-40 which is the formulation expected to release higher portion of calcium ion.

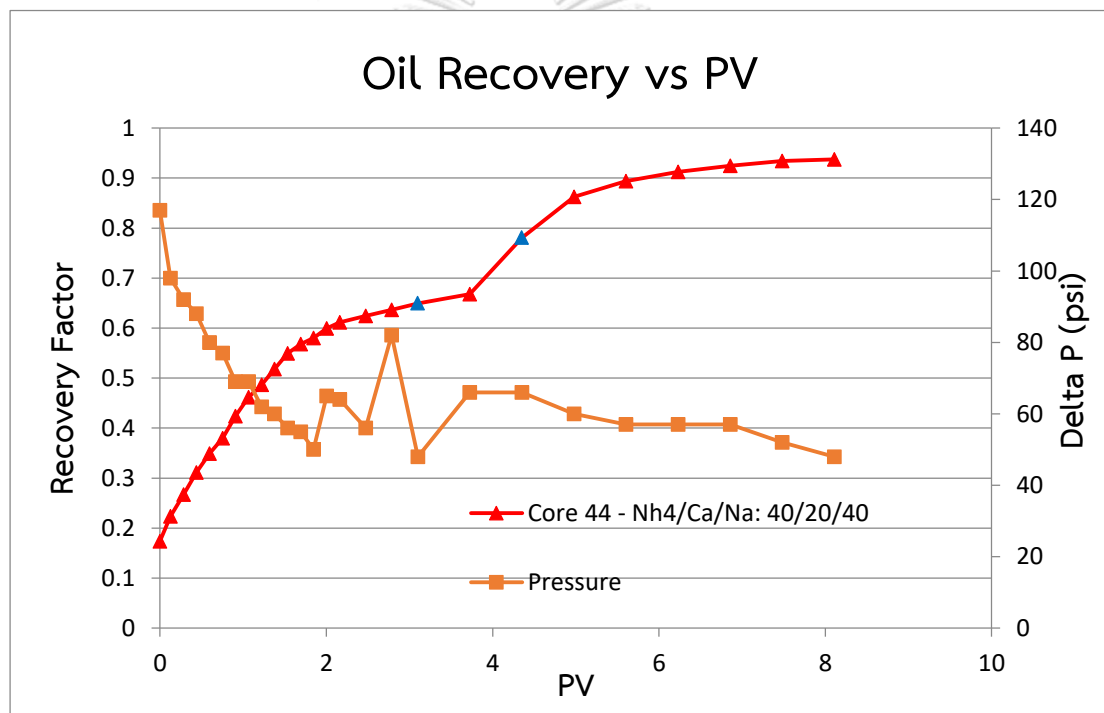


Figure 19 Oil recovery factors from coreflood tests obtained from low salinity water containing ammonium chloride- calcium chloride – sodium chloride at ratio of 40-20-40.

As calcium ion is larger than magnesium ion, the link between rock surface and oil drops is with less strength for the case of calcium ion. By these reasons, the solution expected to release calcium ion tends to yield very good oil recovery. In

this case, the period to observe effect of low salinity water is very short but however, the increase of pressure difference is not obvious. As the core sample no.44 possesses very high permeability (approximately 181 mD) the oil drops liberated from MIE mechanisms therefore, can flow easily without restricting the pore throat and hence, the increment of pressure difference is not obvious. This phenomenon can be explained that the time where conventional flooding was switched to low salinity waterflooding was too soon than it should be and hence, there were still some oil drops liberated during that period, causing fluctuation of pressure during the test. By means of conventional waterflooding, oil recovery is about 76% and after the injection of low salinity water, oil recovery is rapidly increased to 0.94, accounting for 26% incremental by low salinity waterflooding.

In summary, the similarity of case 1 and case 3 is that, both formulation can liberate calcium ion from clay surface and this might be the major reasons to result in a remarkable increment of oil recovery factor. As calcium ion is larger than magnesium ion in terms of ionic size, oil drops that are captured by calcium ion therefore can be liberated easily by these two water formulations. For the case 2 where magnesium ion is more expected, since magnesium ion firmly links between rock surface and oil drops, the liberation of oil therefore occurs difficultly. The presence of ammonium ion is therefore, results in an advantage over potassium ion where it prefers to release magnesium ion instead of calcium ion.

5.4.2 Ion Detections

To observe the effect from MIE process, effluents from coreflooding test are collected and are titrated to identify the amount of calcium ion, magnesium ion, and ammonium ion. Complexometric titration is therefore utilized to identify total hardness and concentration of calcium ion. The amount of magnesium ion is obtained from the difference between total hardness and calcium ion concentration. And the concentration of ammonium ion is obtained from the back titration of sodium hydroxide by hydrochloric acid. Table 14 summarizes the concentration in

ppm of calcium ion, magnesium ion and ammonium ion in the effluents from each test.

Table 14 Summary of titration test after performing coreflooding test

Formulation and Core	Stage	Sample	Ca ²⁺ (ppm)	Mg ²⁺ (ppm)	NH ₄ ⁺ (ppm)
Core 25 Formulation: Pure NH ₄ Cl 1,000 ppm	High	1	160	68	
		2	144	58	
	Salinity Flooding	3	136	58	
		4	120	49	
	Low Salinity Flooding	5	104	15	226
		6	16	0	0
		7	16	0	0
		8	16	0	0
Core 17 Formulation: NH ₄ -Ca-Na 40-40-20 1,000 ppm	High	1	170	91	
		2	110	73	
	Salinity Flooding	3	190	24	
		4	120	0	0
	Low Salinity Flooding	5	20	0	0
		6	20	0	0
Core 44 Formulation: NH ₄ -Ca-Na 40-20-40 1,000 ppm	High	1	192	24	
		2	152	44	
	Salinity Flooding	3	104	58	
		4	64	29	0
	Low Salinity Flooding	5	24	0	0
		6	24	0	0
		7	24	0	0

From Table 14, in the concentration of both calcium ion slightly drops from the value of formation water and magnesium ion is slightly higher than the initial value in formation water during the conventional waterflooding. As calcium ion is consumed to form calcium carboxylic with oil (which is one of the overall MIE mechanism) and also to liberate magnesium ion, amount of calcium ion is therefore, slightly decreased. However, the amount of calcium ion in ppm drops significantly when switching to low salinity waterflooding and being constant afterwards. The amount of magnesium ion in effluent is nearly zero and the amount of ammonium injected in all cases also reduced to zero. It can be explained in the similar direction that ammonium ion tends to replace more calcium ion than magnesium ion. For the case no. 3 where magnesium ion should be more released, magnesium ion that firmly links between rock surface and oil drops therefore, does not tend to be liberated. Some of magnesium ion may also be in the form of magnesium carboxylate complex as magnesium ion can replace calcium ion in a complex with oil at elevated temperature.

In conclusion, results from coreflooding and ion detection can be used to draw some new findings. The selected three low salinity water formulations represented in figure 20 yields different coreflood characteristics. It seems that solely ammonium ion can displace both calcium ion and magnesium ion. However, from stirring test, ammonium tends to favor the dissolution of calcium ion more than magnesium ion. However, the preferable of dissolution can be changed when ammonium is mixed with different ions. For example, when ammonium is mixed with more sodium ion, only dissolution calcium ion is favored and when ammonium ion is mixed with more calcium ion, only dissolution of magnesium ion is favored. From coreflood test, it shows that the function of ammonium ion to cause dissolution of calcium ion is more than that of magnesium ion. Even though adding of potassium ion may shift the dissolution mechanism toward dissolution of magnesium ion, the physical structure between magnesium ion - clay surface - oil drop is not as same as one during the stirring test where oil is nearly absent. Due to smaller ionic size of magnesium ion, it forms a very strong bond between oil and clay surface. This results

in more obvious of oil recovery in case that water formulations tend to favor dissolution of calcium ion than the case of dissolution of magnesium ion.

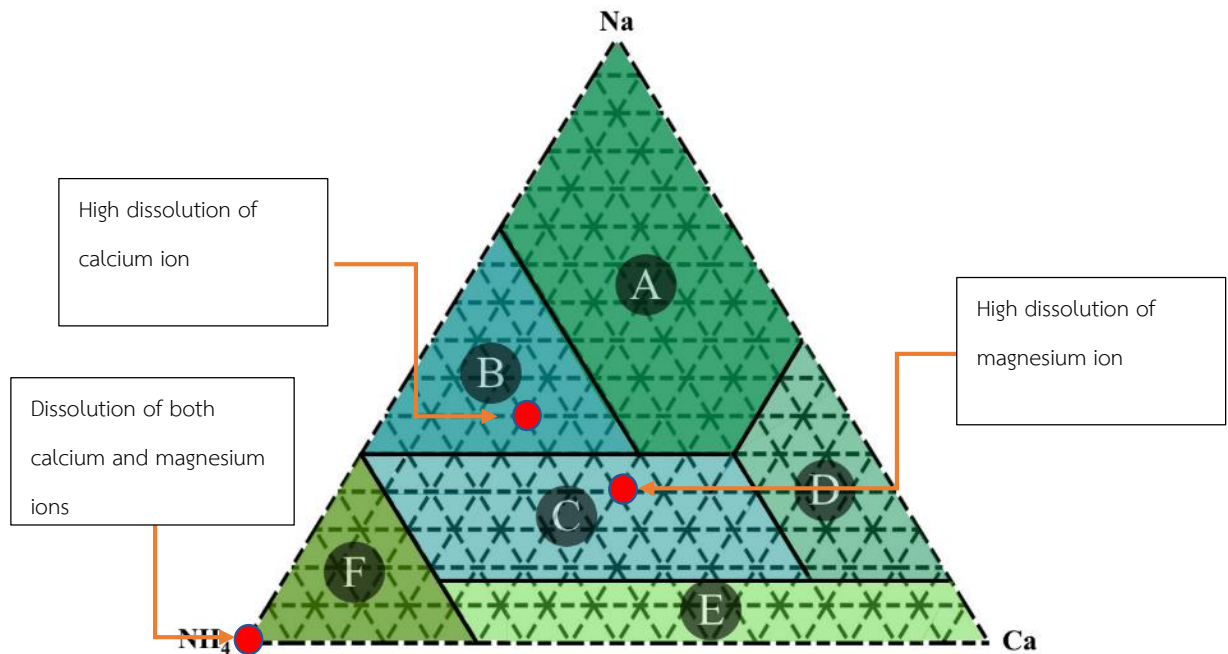


Figure 20 Illustration of dissolution mechanisms for different low salinity water formulations at 1,000 ppm

CHAPTER VI

CONCLUSIONS AND RECOMMENDATIONS

6.1 Conclusions

From the experiments, several conclusions can be made. As ammonium ion is a foreign ion where it does not exist on clay surface, it can be easily adsorbed onto rock surface to displace divalent ions. Nevertheless, the ammonium ion itself tends to displace more calcium ion than magnesium ion on clay surface.

When the concentration of low salinity water is increased, the equilibrium tends to shift. Absent of sodium ion tends to yield benefit for solution with and without ammonium ion as potassium ion may be released from clays to assist the MIE mechanism through the dissolution of magnesium ion.

Adding externally potassium ion into ammonium ion solution shows the shifting from favorability in calcium ion dissolution toward magnesium ion dissolution. However, since the ionic size of magnesium ion is much smaller than calcium ion, divalent ion bridging by magnesium ion is firmly formed and ammonium ion is therefore considered to be superior to potassium ion in oil recovery mechanism since it favors to replace calcium ion.

The results from imbibition and coreflood test confirms that low salinity waterflooding in shaly-sandstone can be accomplished by the used on ammonium ion. However, ammonium ion should be prepared to favor the dissolution of calcium ion since oil that is attached through calcium ion is easier to be recovered compared to that of the dissolution of magnesium ion.

In this study, the solution of pure ammonium chloride and mixture of ammonium-calcium-sodium ion at the ratio of 40-20-40 show good potential in enhancing oil recovery. Nevertheless, the latter case might be more suitable for the existing oilfield since sodium can be mixed with the water formulation at high portion and fresh water demand can be minimized. From the conditions tested in this experiment, oil recovery factor can be increased up to 26 percent.

6.2 Recommendations

In order to get the improvement of this study, potassium ion should be detected throughout the experiment. However, this could result in reduction of number of effluent samplings since more titrations must be conducted. Moreover, iron ion which is enriched in this oilfield and it is also considered as divalent ion should be thoroughly studied.



REFERENCES

1. Alvarez, J.M. and R.P. Sawatzky, *Waterflooding: Same Old, Same Old?*, in *SPE Heavy Oil Conference-Canada*. 2013, Society of Petroleum Engineers: Calgary, Alberta, Canada. p. 18.
2. Sheng, J.J., *Critical review of low-salinity waterflooding*. *Journal of Petroleum Science and Engineering*, 2014. **120**: p. 216-224.
3. Srisuriyachai, F., Suthida, M., Charoentanaworakun, C., Vathanapanich, Y. *Effects of Potassium Ion on Low Salinity Waterflooding in Sandstone Formation*. IOR 2017 - 19th European Symposium on Improved Oil Recovery 2017.
4. Gautier, M., Muller, F., Le Forestier, L., Beny, J. M., Guegan, R., *NH₄-smectite: Characterization, hydration properties and hydro mechanical behaviour*. *Applied Clay Science*, 2010. **49**(3): p. 247-254.
5. Lager, A., Webb, K., J. Black, C. J. J., Singleton, M., Sorbie, K. S., *Low Salinity Oil Recovery - An Experimental Investigation1*. *Petrophysics*, 2008. **49**(01): p. 8.
6. Tang, G.-Q., N.R.J.J.o.P.S. Morrow, and E.V. 24, *Influence of brine composition and fines migration on crude oil/brine/rock interactions and oil recovery*. 1999(2): p. 99-111.
7. Yang, J., Dong, Z., Dong, M., Yang, Z., Lin, M., Zhang, J., Chen, C., *Wettability Alteration during Low-Salinity Waterflooding and the Relevance of Divalent Ions in This Process*. *Energy & Fuels*, 2016. **30**(1): p. 72-79.
8. AlQuraishi, A.A., S.N. AlHussinan, and H.Q. AlYami, *Efficiency and Recovery Mechanisms of Low Salinity Water Flooding in Sandstone and Carbonate Reservoirs*, in *Offshore Mediterranean Conference and Exhibition*. 2015, Offshore Mediterranean Conference: Ravenna, Italy. p. 14.
9. Srisuriyachai, F. and Muchalintamolee, N., *Cation Interference in Low Salinity Water Injection in Sandstone Formation*. 76th EAGE Conference and Exhibition 2014 2014.
10. Pu, H., Xie, X., Yin, P., Morrow, N.R., *Low-Salinity Waterflooding and Mineral Dissolution*, in *SPE Annual Technical Conference and Exhibition*. 2010, Society

- of Petroleum Engineers: Florence, Italy. p. 17.
11. Available from: <https://en.wikipedia.org/wiki/Salinity>.
 12. *Brackish and saline groundwater in New Mexico*. 2015.
 13. Austad, T., *Chapter 13 - Water-Based EOR in Carbonates and Sandstones: New Chemical Understanding of the EOR Potential Using "Smart Water"*, in *Enhanced Oil Recovery Field Case Studies*, J.J. Sheng, Editor. 2013, Gulf Professional Publishing: Boston. p. 301-335.
 14. Apostolos Kantzas, P.P.E., P.P.E. Jonathan Bryan, and P. Saeed Taheri, *Fundamentals of Fluid Flow in Porous Media*. Vol. 4. 2014: PERM's Tomographic Imaging and Porous Media Laboratory.
 15. Available from: <http://perminc.com/resources/fundamentals-of-fluid-flow-in-porous-media/chapter-4-immiscible-displacement/buckley-leverett-theory/>.
 16. Ariani, N., *Data analysis of low-salinity waterflooding to enhance the oil recovery*, in *Petroleum Engineering*. 2018, Missouri University of Science and Technology.
 17. Soraya, B., Malick, C., Philippe, C., Bertin, H.J. and G. Hamon, *Oil Recovery by Low-Salinity Brine Injection: Laboratory Results on Outcrop and Reservoir Cores*, in *SPE Annual Technical Conference and Exhibition*. 2009, Society of Petroleum Engineers: New Orleans, Louisiana. p. 12.
 18. John Wiley & Sons, I., *Ionic Interactions in Natural and Synthetic Macromolecules*. Ion Properties, ed. A.C.a.A. Perico. 2012. p. 1-13.
 19. Available from: [https://chem.libretexts.org/Bookshelves/Physical_and_Theoretical_Chemistry_Textbook_Maps/Supplemental_Modules_\(Physical_and_Theoretical_Chemistry\)/Quantum_Mechanics/09._The_Hydrogen_Atom/Atomic_Theory/Electrons_in_Atoms/Electronic_Orbitals](https://chem.libretexts.org/Bookshelves/Physical_and_Theoretical_Chemistry_Textbook_Maps/Supplemental_Modules_(Physical_and_Theoretical_Chemistry)/Quantum_Mechanics/09._The_Hydrogen_Atom/Atomic_Theory/Electrons_in_Atoms/Electronic_Orbitals).
 20. Available from: <https://commons.wikimedia.org/wiki/File:Na%2BH2O.svg>.
 21. Peter Atkins, J.d.P., *Elements of Physical Chemistry*. 6th ed. 2013, University of Oxford.
 22. Srisuriyachai, F., Vathanapanich, Y., *A Study of Multi-Component Ion Exchange by Ammonium Ion during Low Salinity Waterflooding in Sandstone Formation*,

in *80th EAGE Conference and Exhibition 2018*. 2018, EAGE: Copenhagen.





จุฬาลงกรณ์มหาวิทยาลัย
CHULALONGKORN UNIVERSITY

VITA

NAME Vu Quoc Hung

DATE OF BIRTH 11 December 1993

PLACE OF BIRTH Hanoi, Vietnam

INSTITUTIONS ATTENDED Bachelor of Geological Engineering, Department of Petroleum Geology, Faculty of Oil and Gas, Hanoi University of Mining and Geology

HOME ADDRESS No. 98 Nghi Tam Street, Tay Ho District, Hanoi, Vietnam

PUBLICATION The 13th International Conference on Mining, Materials and Petroleum Engineering (CMMP2019).
The 81st EAGE Annual Conference and Exhibition 2019